

*For submission to Organic Geochemistry*

Final version, 14 August 2012

**Environmental significance of mid- to late Holocene sapropels in Old Man Lake,  
Coorong coastal plain, South Australia: an isotopic, biomarker and  
palaeoecological perspective**

David M. McKirdy <sup>a,\*</sup>, Baruch Spiro <sup>b,1</sup>, Alexander W. Kim <sup>b</sup>, Alan J. Brenchley <sup>c,2</sup>,  
Christopher J. Hepplewhite <sup>c,3</sup>, Antonio G. Mazzoleni <sup>c,4</sup>

<sup>a</sup> Organic Geochemistry in Basin Analysis Group, Centre for Tectonics, Resources and Exploration (TRaX), School of Earth and Environmental Sciences, University of Adelaide, SA 5005, Australia

<sup>b</sup> NERC Isotope Geosciences Laboratory, British Geological Survey, Keyworth, Nottingham NG12 5GG, United Kingdom

<sup>c</sup> Department of Geology and Geophysics, University of Adelaide, SA 5005, Australia

---

\* Corresponding author. Tel: +61 8 8303 8146; fax +61 8 8303 4347

*E-mail address:* [david.mckirdy@adelaide.edu.au](mailto:david.mckirdy@adelaide.edu.au)

<sup>1</sup> Present address: Department of Mineralogy, Natural History Museum, Cromwell Road, London SW7 5BD, United Kingdom

<sup>2</sup> Present address: Geoscience Department, TAFE SA, O'Halloran Hill, SA 5158, Australia

<sup>3</sup> Present address: ACTEW Corporation, Canberra, ACT 2601, Australia

<sup>4</sup> Present address: Optiro Pty Ltd, 50 Colin Street, West Perth WA 6005, Australia

## ABSTRACT

The sedimentary records of the numerous lakes scattered along the seaward margin of the Coorong coastal plain in South Australia attest to the impact of rising sea level and changing climate on their depositional environment. One of the smallest perennial alkaline lakes in the region is Old Man Lake. Originally a topographic low within the Pleistocene–Holocene beach-dune of the Robe Range, it became a brackish water swamp when the Holocene postglacial transgression led to a rise of the local groundwater table; and later, as sea level reached its maximum ~7000 years ago, a restricted embayment of a back-barrier lagoon. Neotectonic uplift eventually led to the isolation of this depocentre from the tidal lagoon, whereupon it entered the final lacustrine phase of its evolution. While the basal paludal to lagoonal sandy unit includes two intervals rich in humic organic matter (OM), it is the 3.7 m-thick upward-shoaling lacustrine succession that is the principal focus of this study. The first of two lacustrine units was deposited beneath an oligo- to mesosaline water column up to 4.5 m deep. It comprises laminated calcareous mud and silt containing charophyte fibres and oogonia and features three discrete layers of dark brown to black sapropel (total organic carbon, TOC = 3–20%) deposited between 3270 and 4910 cal yr BP, a time of increasing regional aridity throughout southeastern Australia and rapid global climate change. The uppermost lacustrine unit, deposited in shallower water, comprises organically lean carbonate mud heavily bioturbated and pelletised by a gastropod fauna, with benthic foraminifera that signal increased salinity of the lake. Five cores taken from the lake provided 20 sections of organic-rich sediment for isotopic characterization of their micritic carbonate ( $\delta^{13}\text{C}_{\text{carb}}$ ,  $\delta^{18}\text{O}_{\text{carb}}$ ) and co-existing OM ( $\delta^{13}\text{C}_{\text{org}}$ ); TOC analysis and Rock-Eval pyrolysis; isolation and GC-MS analysis of their free aliphatic hydrocarbons; and GC-*ir*MS analysis of their  $\text{C}_{23+}$  *n*-alkanes and  $\text{C}_{25:1}$  highly branched isoprenoid (HBI) alkane. The oxygen isotope composition of the carbonate (relative to V-PDB) ranges from –0.1 to +1‰ in the humic facies and from +1 to +3‰ in the sapropelic facies, suggesting an overall increase in degree of evaporation with time. Of the three sapropels, the middle one was deposited in the most evaporated water, an inference confirmed by salinity-related variations in the ostracod population. The carbon isotopic composition of the carbonate in both facies is mostly between –3 and +3‰. Higher values (+4 to +10‰) indicative of methanogenesis are confined to the upper

sapropel layer at the periphery of the lake. The values of  $\delta^{13}\text{C}_{\text{org}}$  range from  $-27$  to  $-24\text{‰}$  in the humic sediments, and from  $-22$  to  $-17\text{‰}$  in the sapropels, indicating the dominance of material of higher plant and algal origin, respectively. For each 'sapropel event' high productivity of diatoms and green (including charophyte) algae in the epilimnion was the principal driver of the accumulation and preservation of OM in such high concentrations. A localised anoxic methanogenic hypolimnion first developed in the centre of the lake during deposition of the middle sapropel. Similar eutrophic conditions accompanied the formation of the upper sapropel, but only around the shallower margins of the lake where the inflow of freshwater from springs facilitated the development of meromixis and accelerated the onset of bacterial methanogenesis. The precursor algal blooms were most likely triggered by the influx of fresh water following winter rainfall. The combination of kerogen hydrogen index and  $\delta^{13}\text{C}_{\text{carb}} - \delta^{13}\text{C}_{\text{org}}$ , previously employed to track secular changes in the record of algal productivity and organic preservation, proved useful in identifying synchronous geographic differences in these processes across the lake. The middle sapropel marks a temporary drop in productivity, during which the abundance of diatoms declined relative to green algae, as interpreted from the ratio  $\text{C}_{25:1} \text{HBI} / \text{C}_{31} n\text{-alkane}$  and the extent of  $^{13}\text{C}$ -depletion in the total OM. HBI alkanes ( $\text{C}_{25:1} \gg \text{C}_{20:0}$ ) are prominent components of the free aliphatic hydrocarbons in the sapropels, confirming the significant contribution of diatoms to their OM. The C-isotopic signatures of the principal  $\text{C}_{25:1}$  HBI isomer and the co-occurring  $\text{C}_{23}\text{--}\text{C}_{31}$  odd carbon-numbered *n*-alkanes further document the non-uniformity of biomass preservation within the middle sapropel and highlight the difference between it and the other two sapropel layers on the southwestern margin of the lake. Sapropel deposition in Old Man Lake occurred between 4100 and 2600 cal yr BP, coinciding with two periods of rapid global climate change characterized by cool poles and dry tropics. The evidence from this study suggests that seasonal algal blooms and meromixis, although not necessarily an anoxic hypolimnion, are required for sapropel formation in the Holocene lakes of the Coorong region. Higher-resolution sampling, dating and comparative analysis (microfossil, biomarker and isotopic) of all these sapropels, is required to establish their collective significance for the regional palaeoclimate record of southeastern South Australia.

Key words: Old Man Lake, Coorong, South Australia, sapropel, diatoms, green algae, ostracods, highly branched isoprenoids, *n*-alkanes, carbon isotopes, compound-specific isotope analysis, palaeoproductivity

## 1. Introduction

The Holocene sedimentary records of shallow ephemeral and semi-permanent lakes scattered along the seaward margin of the Coorong coastal plain in South Australia (Fig. 1) display large and, in part, contrasting variations that attest to the impacts of neotectonic uplift, and changing sea level and climate, on their individual physiographic settings (von der Borch and Altmann, 1979; Rosen et al., 1988; Warren, 1990, 1994; Barnett, 1994; McKirdy et al., 1995, 2002, 2010a; Mee et al., 2004, 2007; Edwards et al., 2006). Significant biogeochemical changes also have been documented in the Holocene estuarine sediments of the Coorong lagoon itself (e.g. Krull et al., 2009; McKirdy et al., 2010b and references cited therein). A prominent feature of many of these shoaling-upwards lacustrine successions is the presence of one or more sapropels, discrete gelatinous calcareous mudstone units up to 1 m thick and rich in organic matter of algal and bacterial origin (total organic carbon, TOC = 2–20%; hydrogen index, HI = 300–900 mg hydrocarbons/g TOC). Given that similar sapropels in deep-lake and marine settings across the globe had been linked to abrupt environmental change, notably increased rainfall and river discharge (e.g. Bouloubassi et al., 1999; Meyers and Lallier-Vergas, 1999; Tolun et al., 2002), it seemed reasonable to consider the possibility that the lacustrine sapropels of the Coorong might likewise be proxies for Holocene climate change (McKirdy et al., 2002). Subsequent radiocarbon dating of examples from North Stomatolite Lake (part of the Salt Creek lake chain), Lake Amy and Old Man Lake, and comparison of their ages with the water-level curve for volcanic maar Lake Keilambete in western Victoria (Fig.1), revealed that they were deposited during a shift to drier conditions across southeastern Australia between 6000 and 2000 yr BP (Mee et al., 2007), coinciding with several periods of rapid global climate change to more arid tropics (Mayewski et al., 2004). Thus, unlike their deep-lake and marine counterparts, the Coorong's shallow lacustrine sapropels appear not to have formed during times of high precipitation and stable, equable climate. The influx of aeolian dust carrying essential nutrients such as silica, phosphate and iron from the dune fields of the

nearby Mallee region (Pell and Chivas, 1995) has been suggested as a possible trigger for the precursor algal blooms (Mee et al., 2007). However, preliminary XRD analysis of the sapropelic mudstone interval in a single core from Old Man Lake (Mee, 2008) revealed only low levels of quartz (<5%) and no evidence of phosphate and iron-bearing minerals.

In order to better understand the origin and palaeoenvironmental significance of the aforementioned sapropels, one of the smallest perennial lakes in the region, Old Man Lake, was chosen for further study because its Holocene succession includes three discrete sapropel units, as well as two underlying humic units. Also known as Little Dip Lake (see e.g. Cann et al., 1999), it is located within the Holocene–Pleistocene beach-dune of the Robe Range that forms the present-day coastline between Robe and Beachport (Fig.1). The next dune inland, the Woakwine Range, was deposited at ~120,000 yr BP during the last interglacial high stand of sea level. Originally a topographic low within the Robe Range, Old Man Lake became a brackish water swamp when the Holocene postglacial transgression led *inter alia* to a rise of the local water table. As sea level neared its maximum ca 7000 yr BP (Belperio, 1995), ocean water inundated the Robe-Woakwine interdunal corridor and Old Man Lake became a restricted embayment of the resultant back-barrier lagoon. Regional neotectonic uplift of ~0.07 mm/yr eventually led to the isolation of this depocentre from the tidal lagoon, whereupon it entered the saline lacustrine phase of its evolution. Like the majority of the Coorong lakes, Old Man Lake is alkaline and fed by sluggish, westward flowing meteoric groundwater (Holmes and Waterhouse, 1983; Warren, 1990). Its small size (area ~3 ha; maximum summer water depth ~2.5 m) renders it particularly sensitive to both short and longer-term environmental change. Thus, for example, the present-day salinity of the lake (20–38 g/L TDS: Henderson, 1997) is subject to seasonal freshening from winter rainfall and local run-off. At nearby Kingston (Fig. 1) maximum annual rainfall is 600 mm and precipitation currently exceeds evaporation for 3–4 months of the year (Mee et al., 2007).

Several other pertinent palaeolimnological features of Old Man Lake have already been reported. Cathodoluminescence studies of its living and recently dead aragonitic gastropods (*Coxiella* spp.) and their skeletal fragments within the thrombolite on its northeastern shore (Fig. 2) luminesce bright green, whereas the same species from the

nearby hypersaline Coorong lagoon displays no luminescence, highlighting the Mn content and lower salinity of the groundwater feeding the lake (Mazzoleni et al., 1995). Highly branched isoprenoids ( $C_{25:1} > C_{20:0}$ ) are prominent among the free aliphatic hydrocarbons in its sapropels, signifying the contribution of diatoms to their precursor microbial biomass (McKirdy et al., 1995, 1999). The elemental and isotopic compositions ( $C/N$ ,  $\delta^{13}C$ ,  $\delta^{15}N$ ) and  $^{13}C$ -nuclear magnetic resonance (NMR) spectra of their bulk organic matter confirm its derivation from lacustrine algae and bacteria, augmented by minor inputs of allochthonous terrestrial vegetation (Mee et al., 2004).

In the present study, a consortium of geochronological, organic geochemical, isotopic and biostratigraphic methodologies was employed to analyse samples ( $n = 22$ ) from the five organic-rich horizons in Old Man Lake. The nature and C-isotopic composition of the organic matter (humic *versus* sapropelic); the distribution of specific acyclic alkane/alkene biomarkers and their C-isotopic signatures; the C and O-isotopic compositions of co-existing micritic carbonate; and the ecological affinities of the lake's fossil ostracod and diatom assemblages have been assembled to better constrain its Holocene depositional history. A specific aim was to elucidate the controls on sapropel formation and to establish the extent of environmental change during the ~1500 year period in which the three sapropels accumulated.

## **2. Analytical methods**

### *2.1 Coring and sampling*

Core 1 (80 mm diameter) and a second core at the same site (AJB OM-1) were recovered with a Wacka Vibracorer. The degree of sediment compaction in the cores was 20%. Four additional cores from elsewhere in the lake (Fig. 2) were taken by manually driving lengths of PVC pipe (50 mm internal diameter) into the lake floor with a slip hammer. This procedure resulted in much greater compaction of the retrieved sediment (*viz.* 65% in cores 2–5: Mazzoleni, 1993). Upon return from the field, the sealed cores were stored in a cold room at 4°C until required. The tube was longitudinally sectioned using a cradle and circular saw, and the sediment core split into halves by drawing a wire along the cuts. Sub-sections of half core from each

sapropel and humic unit penetrated at the aforementioned sites were freeze dried in preparation for their geochemical analysis.

## 2.2 *Radiocarbon dating*

Two sapropel samples (5 cm lengths of quarter core) from AJB OM-1 (Fig. 3) were submitted to the University of Waikato Radiocarbon Dating Laboratory, New Zealand, for dating of their bulk organic matter. The samples were washed in hot 10% HCl, rinsed and dried prior to analysis. The resulting conventional radiocarbon dates, expressed with a  $\pm 1\sigma$  error, were converted to calendar years by calibration against the SHCal04 southern hemisphere atmospheric  $^{14}\text{C}$  curve (McCormac et al., 2004) using the online program, OxCal v. 4.1.7 (Bronk Ramsey, 2010).

## 2.3 *Microfossil isolation and mineralogy*

Fifteen sediment samples spanning the entire length of core AJB OM-1 (Fig. 4) were processed using a procedure similar to that employed by Edwards et al. (2006) and the resulting slides examined by optical microscopy to identify and quantify their ostracod populations. Ostracods were identified by reference to DeDeckker and Geddes (1980), DeDeckker (1981, 1988), Martens (1985) and Yasini and Jones (1995).

The mineralogy of each sample was determined using a Philips PW1050 diffractometer fitted with a graphite monochromator, cobalt  $K\alpha$  radiation (wavelength 1.7902 Å) and a  $2\theta$  scanning range of 3–75° at a step interval of 0.05°. Peaks were identified using the CSIRO XPLOT program and its JCPDS option. The relative proportions of the three principal minerals, aragonite, calcite and quartz were determined using the equations of von der Borch (1976).

Freeze-dried sediment (2 g) from the middle sapropel unit in Core 3 was placed in a centrifuge tube, covered with distilled water (10 mL) and treated with concentrated nitric acid (35 mL) at 60°C for 48 hr with frequent stirring. After centrifuging, the residue was repeatedly rinsed with distilled water until the supernatant was no longer acidic (pH ~6). Separate portions of the dried final residue were mounted on a glass slide for optical microscopy and a stub for scanning electron microscopy (SEM), with

a view to photographing its contained diatoms. The former mount was examined using a Zeiss Photomicroscope III in auto exposure mode and 100 ASA colour slide film. After coating with palladium and gold, the latter mount was examined with a Philips XL 20 scanning electron microscope housed in the Centre for Electron Microscopy and Microstructure Analysis (CEMMSA) at the University of Adelaide. Selected SEM images ( $n = 7$ ) were then sent to Dr David Thomas (Department of Botany, University of Tasmania) for taxonomic identification of the diatoms.

#### 2.4 *Carbonate and organic carbon analysis and Rock-Eval pyrolysis*

The total carbonate and organic carbon contents of dried sediment samples were measured in the School of Earth Sciences, Flinders University, using a LECO carbon analyzer, while aliquots of the same samples were submitted to AMDEL Petroleum Services, Adelaide, for Rock-Eval pyrolysis.

#### 2.5 *Stable isotope analysis*

For the determination of the carbon and oxygen isotope composition of the bulk carbonate in the dried sediment, samples were prepared according to the method of McCrea (1950). The  $\text{CO}_2$  was analysed in a modified VG 903 dual inlet gas source mass spectrometer. Results are reported relative to the V-PDB standard with overall analytical reproducibility better than 0.07‰ for both  $\delta^{13}\text{C}$  and  $\delta^{18}\text{O}$ . The carbon isotopic composition of the bulk organic matter was carried out using a Carlo Erba Elemental analyser coupled via a ConFlo interface to a VG Optima gas source mass spectrometer. Precision was better than 0.3‰ and accuracy was checked against IAEA-CH-7 polyethylene ( $\delta^{13}\text{C} = -31.8\text{‰}$ , V-PDB). All these analyses were undertaken at the British Geological Survey, Keyworth, UK.

#### 2.6 *Extraction and isolation of aliphatic hydrocarbons*

Powdered freeze-dried sediment samples (8–55 g) from selected sapropelic ( $n = 7$ ) and humic ( $n = 3$ ) intervals in cores 1-5 were extracted in Soxhlet apparatus with an azeotropic mixture of dichloromethane and methanol (87:13) for 24 hr. Activated copper turnings were added to the solvent flask to remove any co-extracted elemental sulphur. Upon subsequent removal of solvent in a rotary evaporator, the recovered extractable organic matter (EOM) was separated into its aliphatic hydrocarbon,



aromatic hydrocarbon and polar fractions by conventional open-column liquid chromatography on activated alumina and silica, eluting respectively with petroleum ether; petroleum ether and dichloromethane (40:60); and dichloromethane and methanol (35:65). All solvents were AR grade and distilled prior to use.

## 2.7 GC-FID

Initial GC-FID screening of the isolated aliphatic hydrocarbon fractions was conducted using a Varian 3400 gas chromatograph fitted with a 30 m x 0.25 mm i.d. fused silica column (DB-1, methylsilicone stationary phase, 0.25  $\mu\text{m}$  film thickness) operated in on-column injection mode. Hydrogen was used as the carrier gas at a flow rate of 0.9 ml min<sup>-1</sup>. The oven was temperature-programmed from 60 to 300°C at 4°C min<sup>-1</sup> and held at 300°C for 20 min.

## 2.8 GC-MS

GC-MS analysis of the aliphatic hydrocarbons was undertaken using a Varian 3400 gas chromatograph coupled to a Finnigan TQS-70 quadrupole mass spectrometer at the Australian Wine Research Institute, Urrbrae, South Australia. The gas chromatograph was fitted with a 60 m x 0.25 mm i.d. fused silica column (DB-1, methylsilicone stationary phase, 0.25  $\mu\text{m}$  film thickness). Helium was used as the carrier gas at a flow rate of 0.9 ml min<sup>-1</sup>. Samples in *n*-hexane were injected using a split/splitless injector operated in the split mode (ratio 20:1) at 300°C. The oven was temperature-programmed from 50–120°C at 8°C min<sup>-1</sup> and 120–300°C at 4°C min<sup>-1</sup> then held at 300°C for 30 min. Normal and isoprenoid alkane distributions were determined from the total ion current (TIC) chromatogram, and triterpenoid and  $\Delta^2$ -sterene distributions from the *m/z* 191 and *m/z* 215 ion chromatograms, respectively. Individual biomarkers were identified on the basis of their retention times and mass spectra.

## 2.9 GC-irMS

Compound-specific isotope analysis (CSIA:  $\delta^{13}\text{C}$ ) targeted the most abundant compounds in the silicalite adduct of the aliphatic hydrocarbon fraction (viz. a C<sub>25:1</sub> HBI alkene and the odd-carbon-numbered *n*-alkanes) isolated from the upper, middle and lower sapropel units.

Gas chromatography-isotope ratio mass spectrometry (GC-*ir*MS) was performed at the British Geological Survey, Keyworth, using a Thermoquest (Carlo Erba 8000) GC coupled to an Optima isotope ratio mass spectrometer via a Micromass Isochrom combustion interface. The GC was fitted with a Chrompak CP-SIL 5CB-MS column (60 m length x 0.32 mm i.d. x 0.25  $\mu$ m film thickness) and a split/splitless injector. The carrier gas was helium at a head pressure of 27 psi, producing a flow rate of 2 ml/min at 200°C. Sample injection was done in splitless mode for 1 min (injector temperature = 300°C). Adducts and standards were dissolved in *n*-hexane and co-injected with 1  $\mu$ L of an internal standard (squalane or phenanthrene- $d_{10}$ ). The GC oven was programmed from 40°C (10 min) to 320°C at 10°C/min and held isothermal at 320°C for 10 min. Chromatographically separated compounds were combusted at 850°C; and their isotopic compositions determined by integration of the ion currents of masses 44 and 45.

Before and after the analysis of each sample, the GC-*ir*MS system was tested for stability using commercially available standard C<sub>20</sub> and C<sub>28</sub> *n*-alkanes (Chiron AS®) with certified  $\delta^{13}\text{C}$  values of -33.06 and -29.85‰, respectively. The corresponding values obtained from replicate analyses (n = 9) in the present study were -33.07 and -30.57‰, with reproducibilities of  $\pm 0.44$  and  $\pm 0.54$ ‰. All carbon isotopic ratios are reported relative to the V-PDB standard.

### 3. Results and discussion

#### 3.1 *Lithofacies and macrobiota*

The lithofacies and mineralogy of the upper part of the Holocene succession in Old Man Lake are summarised in Fig. 3 where three distinct lithostratigraphic units are defined.

A basal *upwards-shoaling lagoonal unit* of very fine to coarse-grained quartz-bioclastic carbonate sand and carbonate mud (aragonite > high Mg-calcite > quartz) was deposited unconformably on Pleistocene calcreted aeolianite. Thickening from

east (core 1) to west (cores 4 and 5), its upper part contains a characteristic shallow marine molluscan fauna, comprising the gastropods *Clanculus (Isoclanculus) dunkeri*, *Batillaria diemenensis*, *Hydrococcus brazieri* and *Diala lauta* and the bivalves *Katelysia* sp., *Tellina albinella*, *Ostrea angassi* and *Spisula (Notospisula) trigonella*. The very fine-grained sand at the base of this unit lacks the aforementioned shelly fauna but contains two intervals rich in humic OM (lower, 1–2% TOC; upper, 14–29% TOC: Table 2), signifying initially brackish conditions more conducive to the growth of aquatic vegetation. A well-developed peat layer within the equivalent unit at nearby Lake Amy, also within the Robe Range (Fig. 1), has been dated at  $7870 \pm 210$  cal yr BP (Cann et al., 1999).

Overlying the shallow marine lagoonal facies is a *deep-water (3.5–4.5 m), predominantly saline lacustrine unit* of cream to orange-brown laminated mud and silt containing charophyte fibres and oogonia. Spectacular features of this unit are three discrete layers of dark brown to black sapropelic mud (TOC = 3–20%). Their uncompacted thickness varies according to location, ranging from 6–9 cm on the northeastern margin (core 1) to 20–37 cm in the centre of the lake (core 2). The respective average thicknesses of the lower, middle and upper sapropel layers are as follows: 20, 15 and 14 cm. The upper and lower sapropels from this unit have been dated at  $3270 \pm 70$  and  $4910 \pm 65$  cal yr BP, respectively (Table 1), making them among the youngest so far identified in the Coorong region (Mee et al., 2007). Various thin calcitic hardgrounds occur throughout the sapropel intervals of this unit, and may be attributed to uptake of dissolved CO<sub>2</sub> by benthic microbial communities (including cyanobacteria and diatoms), charophytes and aquatic plants.

The uppermost part of the cored Holocene succession in Old Man Lake is a *shallow-water lacustrine unit* of cream-brown, bioturbated, pelletal, carbonate mud (predominantly aragonite), with minor to abundant remains of the gastropod *Coxiella striata*. The benthic foraminifera *Quinqueloculina* sp., *Elphidium* sp. and *Ammonia* aff. *aoteana* (formerly *becarii*) signal increased salinity of the lake (Cann and DeDeckker, 1981).

### 3.2 *Ostracod and diatom biostratigraphy and palaeoecology*

In their study of ephemeral North Stromatolite Lake, located further north along the Coorong coastal plain in the Salt Creek lake chain (Fig. 1), Edwards et al. (2006) demonstrated the effectiveness of fossil diatoms and ostracods in constraining the salinity and redox of the lake's water column during the accumulation of its sapropel unit which attained a thickness of up to 2 m in the deeper hollows of the lake. In the present study of Old Man Lake, the small number of samples examined for diatoms contained relatively few intact frustules, the majority being corroded or partially dissolved. Only two taxa, both benthic, have been identified in the middle sapropel of Core 3: *Campylodiscus clypeus* (dominant) and *Pinnularia* sp. (frequent). The former is well adapted to brackish conditions, while the latter is likely to be a saline species (D.E. Haynes, pers. comm., 2012). Delicate pennate individuals like the *Pinnularia* sp. illustrated in Hepplewhite (1994) may be more susceptible to dissolution in alkaline porewater than the larger, more structurally robust *Campylodiscus* sp. (Edwards et al., 2006). The pH of modern pore water (measured at 2 cm depth in the sediment column) varies seasonally between 7.6 and 8.3 (Henderson, 1997), conditions inimical to the preservation of diatom frustules. Thus, the apparent dominance of *Campylodiscus* in the middle sapropel of Old Man Lake, and the depauperate nature of its fossil diatom assemblage, may be artefacts of early diagenesis. The usefulness of this two-pronged micropalaeotological approach to the study of the sapropels in Old Man Lake is therefore weakened. Diatoms are much better preserved in the sapropel unit of North Stromatolite Lake with up to 20 benthic species identified in any one sample. Here stratigraphic variation of the proportions of key indicator species reveals a marked oscillation between oligosaline and eusaline conditions (1.6–40 g/L TDS) in the hypolimnion during its ~1200 yr period of sapropel deposition (Edwards et al., 2006).

In marked contrast to diatoms, fossil ostracods are both more abundant and more diverse at Old Man Lake, as shown in the biostratigraphic profile of core AJB OM-1 (Fig. 4). The number of individual valves per sample increases up section from 18–98 in the lagoonal unit, through 78–278 in the laminated lacustrine unit, to 196–356 in the massive lacustrine unit. A total of nine species have been identified. In terms of their palaeoecological affinities, the ostracod assemblages confirm the evolution of the lake's setting from restricted marine to brackish-saline lacustrine. Of particular significance is the coincidence of the epiphytic freshwater species *Limnocythere*

*mowbrayensis* with all three sapropel intervals. This suggests that the sapropels are products of algal blooms triggered by freshening of the hypolimnion during periods of atypically high rainfall and enhanced local runoff. Obviously there are other contributing factors since the relative abundance of *L. mowbrayensis* in the middle sapropel is appreciably lower than in the other two sapropels, perhaps indicating a temporary reversal of the trend to lower salinity. Another interesting feature of the sapropel-bearing interval of the laminated lacustrine unit is the steady rise in the relative abundance of the large planktonic species *Mytilocypris praenuncia*, arguably in response to a rising water table and consequent deepening of the lake.

### 3.3 Organic facies

Two contrasting organic facies are present within the Holocene succession at Old Man Lake (Tables 2 and 3, Fig. 3). Carbonaceous sands in the lagoonal unit contain humic Type III organic matter (HI = 108–210;  $\delta^{13}\text{C}_{\text{org}} = -27$  to  $-24\text{‰}$ ), whereas that in the organic-rich layers of the laminated lacustrine unit is of sapropelic Type II composition (HI = 278–800;  $\delta^{13}\text{C}_{\text{org}} = -22$  to  $-17\text{‰}$ ). In terms of their organic richness and kerogen type (Fig. 5) and their bulk C-isotopic composition, these thin sapropels overlap the much thicker and somewhat older sapropel in North Stromatolite Lake (HI = 323–925;  $\delta^{13}\text{C}_{\text{org}} = -22$  to  $-16\text{‰}$ ; Mee et al., 2004; McKirdy et al., 2010a). The extent of  $^{13}\text{C}$  depletion in these two organic facies is consistent with their origin from mainly higher plant and algal/cyanobacterial precursors, respectively. Although a detailed palynological study of these sediments has yet to be undertaken, lacustrine sapropels of similar age elsewhere on the Coorong coastal plain, at North Stromatolite Lake and in a former embayment of Lake Alexandrina at the terminus of the River Murray (Fig. 1), have been shown to incorporate the remains of bacillariophyceae (diatoms), chlorophyceae (green algae, including *Botryococcus* sp.) and cyanobacteria, along with lesser amounts of cuticle and pollen (von der Borch and Altmann, 1979; McKirdy et al., 2010a).

Regardless of core location in Old Man Lake, the organic matter in the middle sapropel is isotopically lighter than that in both the lower sapropel (by  $\sim 1\text{‰}$ ) and the upper sapropel (by  $\sim 3\text{‰}$ ). This observation appears to be at odds with the

aforementioned apparent higher salinity of the lake water during deposition of the middle sapropel, and may indicate a change in the balance of biota contributing organic matter to the lake floor. For example, it is now well established that marine bloom-forming diatoms are on average 6‰ heavier than their associated phytoplankton and particulate OM (Fry and Wainwright, 1991; Tyson, 1995). Accordingly, Ariztegui et al. (2001) invoked the enhanced productivity of diatoms (relative to cyanobacteria) to explain a positive  $\delta^{13}\text{C}_{\text{org}}$  excursion in diatom-rich units of the Holocene succession in Lake Albano, Italy. Thus, the middle sapropel may have recorded the opposite effect, viz. a decrease in the ratio of diatom to green algal productivity.

The yields of EOM from the lacustrine sapropels in Old Man Lake (4377–10945 ppm, dry wt; 56–117 mg/g TOC), while typically higher than those for the underlying lagoonal humic sands (494–8367 ppm; 22–60 mg/g TOC), are somewhat lower than those obtained from the sapropel in North Stromatolite Lake (10072–14594 ppm; 105–160 mg/g TOC: McKirdy et al., 2010a). The latter difference may reflect the better preservation of microbial biomass beneath a deeper hypolimnion at the northern locality (mean HI = 617 at NSL; cf. 502 at OML). The laminated texture of the host sediment in both depocentres attests to the absence of bioturbation. In North Stromatolite Lake, this exclusion of grazing and burrowing macrofauna from the sapropel was not due to perennial bottom water anoxia. Citing the existence of a flourishing benthic ostracod community, and the intact valve ornamentation of one of its constituent taxa *Osticythere baragwanathi* (Yasini and Jones, 1995), Edwards et al. (2006) argued that the lake floor was at all times well oxygenated. *O. baragwanathi* is not part of the fossil ostracod assemblage in Old Man Lake.

### 3.4 Carbonate isotope signatures

The C and O-isotopic compositions of micritic carbonate in the organic-rich sediments of Old Man Lake are summarised in Table 2 and plotted in Fig. 6.  $\delta^{18}\text{O}$  of the carbonate is a bulk indicator of the water source. Values range from –0.1 to +0.8‰ in the humic facies, and from +1 to +3 ‰ in the sapropelic facies. Overall, the carbonates in the organic-rich layers have compositions similar to or heavier than that

of seawater, and an overall increase in degree of evaporation with time can be recognised. Of the three sapropels, the middle one was deposited in the most evaporated water, an inference confirmed by salinity-related variations in the ostracod population (Fig. 4).

$\delta^{13}\text{C}$  of the same carbonate is mostly between  $-3$  and  $+3\text{‰}$  for both organic facies (Table 2). Higher values ( $+4$  to  $+10\text{‰}$ ), indicative of precipitation of the  $^{13}\text{C}$ CO<sub>2</sub> coproduced by methanogenic archaeobacteria during the diagenesis of organic-rich sediments (Irwin et al., 1977; Talbot and Kelts, 1990), are confined to the upper sapropel layer at the periphery of the lake. The latter feature is associated with a fall in the lake level and the inflow of water from freshwater springs along the western side of the lake, which in turn lowers the sulfate content of the hypolimnion and hastens the onset of methanogenesis. The springs are sites of abundant reed growth. Similar springs are located on the western shores of other lakes, including Lake Amy (Fig. 1), in the Robe Range.

### 3.5 *Aliphatic hydrocarbons*

The lacustrine sapropels of Old Man Lake contain more free aliphatic hydrocarbons (110–361 ppm dry wt) than do its lagoonal humic sands (20–268 ppm). While they comprise  $<4\%$  of the extractable OM and represent only a minor portion of the total sedimentary OM (1–4 mg/g TOC), such geolipids and their C-isotopic signatures nevertheless provide useful clues to the sources of that OM (Meyers, 2003; Mead et al., 2005; McKirdy et al., 2010b).

TIC chromatograms of the aliphatic hydrocarbons isolated from representative samples of lagoonal humic and lacustrine sapropelic sediment are compared in Fig. 7. Selected biomarker parameters derived from these and the other samples so analysed are presented in Table 3. Irrespective of organic facies, the chromatograms are dominated by *n*-alkanes ranging from C<sub>12</sub> to C<sub>35</sub>, skewed in abundance towards higher carbon numbers, and displaying a marked predominance of odd-carbon-numbered homologues beyond C<sub>22</sub> (CPI = 3–17). In all but one sample, *n*-C<sub>31</sub> is the most abundant homologue and *Paq*, a molecular proxy for aquatic macrophytes (Ficken et

al., 2000), has values of 0.3–0.5 that straddle the ranges for emergent (0.1–0.4) and submerged/floating (0.4–1) macrophytes. The exception is the upper humic sample from core 5 (maximum at  $n$ -C<sub>25</sub>;  $Paq = 0.83$ ), which appears to contain the highest input of lipids from submerged/floating macrophytes. One such macrophyte presently growing in the lake is *Ruppia* sp. (Mee, 2008), to which similar  $n$ -alkane distributions in Holocene estuarine sediments of the southern Coorong Lagoon have been attributed (McKirdy et al., 2010b). Other than the aforementioned, unidentified reeds confined to the western and northwestern edges of the lake, it hosts no emergent macrophytes.

An  $n$ -alkane distribution pattern such as those in Fig. 7 is usually attributed to terrestrial plants or emergent macrophytes (Eglinton and Hamilton, 1967; Ficken et al., 2000). Additional potential sources of sedimentary long-chain  $n$ -alkanes are certain microalgae (including diatoms, dinoflagellates and chlorophytes: Volkman et al., 1998), cyanobacteria (Gelpi et al., 1970) and sulphate-reducing bacteria (Davis, 1968; Han and Calvin, 1969; Spiro and Aizenshtat, 1977). However, the  $n$ -alkanes and  $n$ -alkenes synthesised by such biota (with the notable exception of the chlorophyte *Botryococcus braunii*, race A: Lichtfouse et al., 1994) lack the pattern of extended odd-carbon-number predominance evident in Fig. 7. Commonly one or two individual homologues (e.g. C<sub>25</sub>, C<sub>27</sub>) are dominant, as in the diatom culture analysed by Volkman et al. (1980). Prepared from an Australian intertidal sediment and comprising *Melosira*, *Biddulphia*, *Nitzschia* and *Navicula* species, its  $n$ -alkane profile is heavily skewed towards lower carbon numbers (<C<sub>21</sub>) and would be unimodal but for the fact that C<sub>25</sub> is the major homologue and therefore dominates the C<sub>23+</sub> range. Likewise, diatoms harvested from Mono Lake, California, yielded a unimodal distribution of C<sub>15</sub>–C<sub>31</sub>  $n$ -alkanes (maximum at C<sub>25</sub>) displaying no odd or even predominance (Henderson et al., 1972).

If algae and bacteria were major sources of the biomass preserved in the sapropels then one might expect non-waxy  $n$ -alkanes (C<sub>12</sub>–C<sub>21</sub>) to figure more prominently among their free aliphatic hydrocarbons (cf. Han and Calvin, 1969; Gelpi et al., 1970; Blumer et al., 1971). Commenting on a similar phenomenon in pelletised cyanobacterial ooze from Mud Lake, Florida, Han et al. (1968, p. 32) surmised that  $n$ -heptadecane (and presumably other short-chain  $n$ -alkanes) might be ‘a particularly



suitable substrate for certain nonphotosynthetic bacteria' which convert them into higher molecular weight hydrocarbons. The absence of another microalgal (including diatom) marker, *n*-heneicosa-3,6,9,12,15,18-hexaene (*n*-C<sub>21:6</sub>), is more readily explained. Being highly unsaturated, it is rapidly degraded and unlikely to survive other than within intact algal cells in surficial sediments (Volkman et al., 1998).

The most obvious feature distinguishing the free aliphatic hydrocarbons in the sapropels from those in the humic sediments is their high relative abundance of C<sub>20</sub> and C<sub>25</sub> highly branched isoprenoids (HBI: Fig. 7). As unambiguous biological markers of the Bacillariophyceae (e.g. Volkman et al., 1994; Belt et al., 2001a,b; Rowland et al., 2001), these compounds confirm the important contribution diatoms have made to the sapropels of Old Man Lake, notwithstanding their dearth of intact frustules. The C<sub>25</sub> HBI, here represented by three isomeric monenes and a diene (Fig. 8), is by far the dominant homologue, while the C<sub>20</sub> HBI 2,6,10-trimethyl-7-(3-methylbutane)-dodecane is present in much lower concentrations (Table 3). This contrasts with the situation in the Holocene sapropelic sediments of an unnamed ephemeral lake near Lake Albert at the mouth of the River Murray (Fig. 1: Hepplewhite, 1994), North Stromatolite Lake (McKirdy et al., 1995, 2010a) and the adjacent southern Coorong Lagoon (McKirdy et al., 2010b), wherein C<sub>20:0</sub> HBI is not only the principal HBI but also the major free alkane. Although this enigmatic biomarker has yet to be identified in any living diatom (Volkman et al., 1998), the circumstantial evidence of its occurrence in a wide variety of Holocene diatom-bearing coastal and lacustrine sediments (e.g. Rowland and Robson, 1990; Belt et al., 2000; Jaffé et al., 2001; Xu et al., 2006; Aichner et al., 2010), some of them notably hypersaline (Dunlop and Jefferies, 1985; Kenig et al., 1989), points to its likely origin from epiphytic diatoms (Atahan et al., 2007; McKirdy et al., 2010b).

In Old Man Lake potential substrates for these inferred epiphytes were the aforementioned *Ruppia* sp., charophyte algae and benthic microbial mats (see section 3.7). Here, however, the pronounced imbalance between the different HBIs (C<sub>25</sub> >> C<sub>20</sub>: Table 3) suggests that epiphytes were only a minor component of the lake's diatom population during sapropel deposition. Their low abundance could imply a paucity of suitable, long-lived substrates. Further clues to the identity of the

sapropels' precursor biota and their palaeoecological inter-relationships are provided by the isotopic signatures of their biomarker hydrocarbons.

### 3.6 *Compound-specific isotopic signatures in sapropels*

The carbon isotopic signatures of the most abundant free aliphatic hydrocarbons in representative samples of sapropel from Old Man Lake (viz. the C<sub>23+</sub> odd carbon-numbered *n*-alkanes and the major C<sub>25:1</sub> HBI) are listed in Table 4 and, along with those of their corresponding total organic carbon ( $\delta^{13}\text{C}_{\text{org}}$ ), are compared in Fig. 9.

Several features are immediately apparent. First, the up-section pattern of isotopic variation identified in the bulk organic matter of core 5 is clearly evident only in the C<sub>27</sub> and C<sub>33</sub> *n*-alkanes (Fig. 9b). Second, the mid-chain *n*-alkanes (C<sub>23</sub> and C<sub>25</sub>) in the middle sapropel of core 5 are isotopically lighter (by 2–3‰) than those in the same sapropels in cores 1 and 2 (Fig. 9a), and those in the lower and upper sapropels from the same locality (Fig. 9b). Third, there is a marked isotopic difference between the C<sub>25:1</sub> HBI and *n*-alkanes in the middle sapropel of core 5.

The  $\delta^{13}\text{C}$  values of individual hydrocarbons fall within the range –33 to –23‰, making them appreciably more depleted in <sup>13</sup>C (by up to 12‰) than the bulk organic matter. The C<sub>25:1</sub> HBI is isotopically heavier than the lightest co-occurring *n*-alkanes in all but the middle sapropel from the centre of the lake (core 2). This enrichment in <sup>13</sup>C is as would be expected for diatom-derived geolipids (e.g. Canuel et al., 1997). Diatoms are typically enriched in <sup>13</sup>C relative to other phytoplankton because they tend to grow in blooms, leading to localised depletion of dissolved CO<sub>2</sub> and reduced discrimination against <sup>13</sup>CO<sub>2</sub> in the resulting C<sub>3</sub> photosynthate, while some species are able to assimilate HCO<sub>3</sub><sup>–</sup> via the C<sub>4</sub> pathway (Freeman et al., 1994). It is worth noting that the C<sub>20:0</sub> HBI and the same *n*-alkanes are 5–10‰ heavier in the organic-rich sediments of the southern Coorong Lagoon, where they reflect the much higher salinity of this estuarine water body (McKirdy et al., 2010b).

The  $\delta^{13}\text{C}$  *versus* carbon number profile of waxy *n*-alkanes isolated from any given photoautotroph is typically smooth and has a negative or zero slope (e.g. Collister et

al., 1994; Chikaraishi and Naraoka, 2003; Mead et al., 2005). The profiles obtained from the sapropels are unusual in that they exhibit a marked positive offset between  $C_{25}$  and  $C_{27}$  (Fig. 9). No such offset is evident in the organic-rich Holocene sediments of Lake Koucha, Tibet (Fig. 10), where the  $C_{23}$  and  $C_{25}$  homologues typically differ by  $<2\text{‰}$  and provide a coherent isotopic signature for saline aquatic macrophytes, which in turn is heavier than that of the  $C_{27}$ – $C_{33}$  *n*-alkanes ( $\delta^{13}\text{C} = -23$  to  $-30\text{‰}$ ) derived from freshwater phytoplankton (Aichner et al., 2010).

Thus, the mid-chain *n*-alkanes (especially *n*- $C_{25}$ ) in the sapropels of Old Man Lake appear to have multiple sources. The  $C_{29}$ – $C_{33}$  *n*-alkanes are isotopically light ( $-28$  to  $-32\text{‰}$ ) consistent with their derivation from green algae. A natural bloom of *Spirogyra* sp., a charophyte green alga commonly found in eutrophic freshwater settings, was shown by Zhang et al. (1999) to contain  $C_{17}$ – $C_{35}$  *n*-alkanes with  $\delta^{13}\text{C}$  values in the range  $-30$  to  $-35\text{‰}$ . In contrast,  $C_{23}$  and  $C_{27}$  are  $\sim 4\text{‰}$  heavier than their adjacent homologues and (except in the middle sapropel from core 5) isotopically similar to the  $C_{25:1}$  HBI, suggesting their origin from diatom lipids.

Another intriguing feature of the  $C_{23}$ – $C_{27}$  *n*-alkanes in the middle sapropel is their progressive enrichment in  $^{13}\text{C}$  down-wind through cores 5, 2 and 1 (Figs. 1 and 9a). This may perhaps be attributed to an enhanced input of floating macrophytes, except for the fact that there is no parallel increase in *Paq* (Table 3). It is more likely a result of enhanced carbonate precipitation along the shallower eastern margin of the lake, limiting the  $\text{CO}_2(\text{aq})$  available to benthic diatoms and giving rise to the thrombolite that crops out along the adjacent lake shore (Fig. 2). But this then begs the question as to why the same isotopic gradient is not also evident in the diatom-specific biomarker,  $C_{25:1}$  HBI (Fig. 9a).

The isotopic signature of the  $C_{25:1}$  HBI is relatively constant in all three sapropels intersected by core 5 ( $\delta^{13}\text{C} = -23.7$  to  $-24.8\text{‰}$ ; Fig. 9b). This indicates that the carbon source tapped by the diatoms involved in sapropel formation on the lake's southwestern margin remained stable and homogeneous for ca 1500 yrs. However, the northeasterly transect of the middle sapropel reveals that this particular biomarker is 2–3‰ lighter in the middle of the lake than at its margin (Fig. 9a). Significantly, the

carbonate content of the middle sapropel deposited in the deepest part of the lake (30%) is less than half that at the shallow lake margins (57–74%: Table 2) where the enhanced precipitation of carbonate would have lessened the ability of diatoms to discriminate against  $^{13}\text{CO}_2(\text{aq})$  during photosynthesis.

### 3.7 *Genesis of sapropel and its possible link to littoral microbialite*

In their study of modern organic-rich sediments in seasonally stratified Lake Greifen, Switzerland, Hollander et al. (1992, 1993) noticed that the isotopic fractionation between coexisting carbonate and organic carbon ( $\Delta^{13}\text{C} = \delta^{13}\text{C}_{\text{carb}} - \delta^{13}\text{C}_{\text{org}}$ ) varied systematically with the HI of the kerogen. This variation was attributed to secular changes in primary productivity and preservation of the resulting algal biomass, and their impact on the  $\text{CO}_2(\text{aq})$  budget of the lake. A negative correlation between HI and  $\Delta^{13}\text{C}$  was taken to implicate high productivity as the main driver of the preservation and accumulation of organic matter, whereas a positive correlation suggested low to moderate productivity accompanied by bottom-water anoxia. Using the eutrophic lake model of Hollander and co-workers as an interpretative template for the HI and  $\Delta^{13}\text{C}$  data from Old Man Lake (Fig. 11), it is clear that there is no uniform lake-wide pattern of secular change in productivity and preservation between the lower, middle and upper sapropels. However, each sapropel unit provides a snapshot of the differing levels of organic preservation at five sites across the lake during prolonged episodes of elevated algal productivity, as evidenced by the three separate trends highlighted in Fig. 11.

All three trends show a negative correlation between HI and  $\Delta^{13}\text{C}$ . Within the lower sapropel the correlation is rather weak (hence the dashed line in Fig. 11), in contrast to the much stronger correlations in the middle and upper sapropels. The relatively tight grouping of data points for the *lower sapropel* points to uniformly high productivity and preservation across the lake at this time: TOC = 7.6–10.3 (mean 8.2) percent; HI = 433–526 (mean 487) mg S2/g TOC. During the subsequent sapropel events this uniformity dissipated as some parts of the lake became much more productive than others, and its centre responded differently to its margins. Thus, in the *middle sapropel*, TOC ranges from 6.0 to 19.6 (mean = 10.3) percent and HI from 334

to 595 (mean = 432) mg S2/g TOC. The southeastern margin of the lake (core 3) was the least productive and the northern margin (core 4) the most productive (Fig. 11). In the deepest central part of the lake, a similarly high level of surface productivity was augmented by the development of an anoxic methanogenic hypolimnion, explaining why the sample from core 2 has the highest TOC and HI values recorded for the middle sapropel (Table 2) and plots off trend in Fig. 11. By the onset of the *upper sapropel* methanogenic conditions had extended to the hypolimnion at the shallower margins of the lake, creating a new regime of enhanced algal productivity and preservation, and where TOC increases from 3.2 to 9.3 (mean 6.3) percent and HI from 449 to 800 (mean = 560) mg S2/g TOC between core sites 1, 3, 4 and 5. Once again, the sample from the deepest part of the lake (core 2) does not conform to the trend defined by those from the peripheral localities (Fig. 11). Its much lower  $\Delta^{13}\text{C}$  value seems to indicate that bottom-water anoxia and methanogenesis were not factors influencing carbon cycling at this time in the centre of the lake. Instead, its high TOC and HI values (viz. 16.4% and 698 mg S2/g TOC: Table 2) would appear to have resulted solely from high productivity in the epilimnion, accompanied by the precipitation of isotopically light carbonate ( $\delta^{13}\text{C}_{\text{carb}} = -0.4\text{‰}$ ) derived from aerobic bacterial decay of particulate OM settling through the upper reaches of the water column. This in turn is entirely consistent with the previously remarked lower carbonate content of the upper sapropel in the centre of the lake (27%, cf. 53–85% at its shallow margins: Table 2).

Each core taken in Old Man Lake (Fig. 2) provides a different history of its palaeoproductivity. Only near the centre of the lake (represented by core 2) is there a regular stepwise increase in HI, which in lacustrine settings is reasonably regarded as a proxy for the preservation of autochthonous microbial biomass. It is here that the sapropels collectively exhibit their highest mean TOC and HI values (14.9% and 575 mg S2/g TOC). In contrast, at core sites 1, 3 and 5, the middle sapropel records an overall drop in such preservation relative to the lower sapropel, before it increases again in the upper sapropel. The least variable location in terms of productivity and preservation is core site 4, while the least productive portion of the lake is its southeastern margin (core site 3).

A raised terrace of indurated thrombolitic carbonate (aragonite and low-Mg calcite) on the eastern shore of Old Man Lake (Fig. 2) records a period of microbialite formation (Brenchley and Gostin, 1998). Originally a gelatinous benthic microbial community (BMC), predominantly diatoms, in which monohydrocalcite had precipitated in response to photosynthetic drawdown of dissolved CO<sub>2</sub>, the microbialite is tentatively interpreted as a shallow-water, shoreline equivalent of the upper sapropel. Thus, the thrombolite terrace represents a "fossil microbialite". A similar phenomenon exists on the present-day floors of saline Lake Lenore and Soap Lake in the state of Washington, USA (Castenholz, 1960). In the deeper parts of both lakes diatoms and cyanobacteria comprise a crumbly gelatinous benthic aggregate, while in the shallower littoral parts of the less saline Lake Lenore diatoms seasonally colonise cyanobacterially-bound microbial mats forming widespread epilithic layers.

Since ~2700 yr BP lake levels in the Robe Range have dropped by up to 2.5 m. A falling water table, combined with sediment accumulation, has reduced the seasonal average depth of many lakes (including Old Man Lake) to less than 3 m at their centre. The uppermost sediments of these lakes consist of bioturbated and pelletised carbonate muds. Deeper lakes subject to marginal freshwater inflow (e.g. Lake Amy, the surface expression of a perched water table) have continued to support BMC's despite falling water levels. Such lakes are currently precipitating monohydrocalcite within nearshore "living microbialites", while their offshore zone is floored by an organic-rich BMC gel. The latter awaits further study aimed at comparing its isotopic and biomarker signatures with those of the Holocene sapropels.

#### **4. Conclusions**

The three thin sapropel units preserved within the ~3.7 m thick Holocene lacustrine succession of shallow perennial Old Man Lake represent sequential extended periods of high seasonal algal productivity between 4910 and 3270 cal yr BP, a time of increasing regional aridity throughout southeastern Australia and rapid global climate change to drier tropics. For each 'sapropel event' high productivity of diatoms and green algae in the epilimnion was the principal driver of the preservation and accumulation of H-rich Type II kerogen. A localised anoxic methanogenic

hypolimnion first developed in the centre of the lake during deposition of the middle sapropel, a time when evaporation exceeded precipitation. Similar eutrophic conditions accompanied the formation of the upper sapropel, but only around the shallower margins of the lake where the inflow of freshwater from springs as a result of a return to wetter conditions facilitated the development of meromixis and accelerated the onset of bacterial methanogenesis.

The combination of kerogen hydrogen index and  $\delta^{13}\text{C}_{\text{carb}} - \delta^{13}\text{C}_{\text{org}}$ , employed by Hollander et al. (1992, 1993) to track secular changes in algal productivity and organic preservation, here proved useful in identifying geographic differences in these processes across the lake. To the best of our knowledge, such lateral variation has not previously been reported in a shallow eutrophic lacustrine setting as small as Old Man Lake. The middle sapropel was deposited during a temporary reversal of the overall trend of increasing productivity. This reversal also saw a decline in the abundance of diatoms relative to green algae, as expressed in the biomarker ratio  $\text{C}_{25:1} \text{HBI} / \text{C}_{31} n\text{-alkane}$  and the extent of  $^{13}\text{C}$ -depletion in the total OM ( $\delta^{13}\text{C}_{\text{org}}$ ).

Highly branched isoprenoid alkanes ( $\text{C}_{25:1} \gg \text{C}_{20:0} \text{HBI}$ ) are prominent components of the free aliphatic hydrocarbons in the sapropels, confirming the significant contribution of diatoms to their organic matter. The compound-specific C-isotopic signatures of the principal  $\text{C}_{25:1} \text{HBI}$  isomer and the co-occurring  $\text{C}_{23}\text{--}\text{C}_{31}$  odd carbon-numbered *n*-alkanes further document the non-uniformity of the biomass preserved within the middle sapropel and highlight the difference between it and the other two sapropel layers on the southwestern margin of the lake. This difference is manifest in its  $\text{C}_{23}$  and  $\text{C}_{25}$  *n*-alkanes (isotopically lighter by 2–3‰), perhaps implying that these mid-chain homologues had multiple sources.

Seasonal algal blooms and meromixis over an extended period (~500 yr), although not necessarily an anoxic hypolimnion, were required for the formation of an individual sapropel unit in Old Man Lake. Elsewhere along the Coorong coastal plain, ostensibly similar mid- to late Holocene sapropels occur in other shallow lakes of differing hydrology, salinity, water chemistry, mineralogy and biota. As these factors, individually or in concert, may potentially influence the production and preservation

of lacustrine organic matter, the same palaeoclimatic significance cannot justifiably be assigned to each local sapropel event. A similar multi-tool approach to that employed in this study, but involving higher-resolution sampling, dating and analysis (microfossil, biomarker and isotopic) of all the aforementioned Coorong sapropels, is required to establish their collective significance for the regional palaeoclimate record of southeastern South Australia.

## **Acknowledgements**

The National Parks and Wildlife Service, South Australian Department for Environment, Heritage and Aboriginal Affairs, granted us permission to undertake coring in the Coorong National Park. This study is based in part on the B.Sc. Honours theses of Christopher Hepplewhite and Tony Mazzoleni and the postgraduate research project of Alan Brenchley. Partial accounts of its findings were presented at the 17th International Meeting on Organic Geochemistry, Donostia-San Sebastián, Spain, the 19th International Meeting on Organic Geochemistry, Istanbul, Turkey and the 16<sup>th</sup> Australian Geological Convention, Adelaide, South Australia. Professor Chris von der Borch (School of Earth Sciences, Flinders University of South Australia) generously offered us access to his coring equipment, core storage and laboratory facilities. Elizabeth Fontaine-Geary, Bernd Michaelsen, Xinke Yu and Tony Hall (University of Adelaide) provided technical support and advice. Dr. David Thomas (Department of Botany, University of Tasmania) kindly undertook the initial diatom identifications. Deborah Haynes (University of Adelaide) updated the diatom identifications, assisted with the OxCal calibrations and helpfully critiqued parts of the penultimate draft of the manuscript. The contribution of DMMcK to this paper forms TRaX Record xxx.



## References

- Aichner, B., Wilkes, H., Herzsuh, U., Mischke, S., Zhang, C., 2010. Biomarker and compound-specific  $\delta^{13}\text{C}$  evidence for changing environmental conditions and carbon limitation at Lake Koucha, eastern Tibetan Plateau. *Journal of Paleolimnology* 43, 873–899.
- Ariztegui, D., Chondrogianni, C., Lami, A., Guilizzoni, P., Lafargue, E., 2001. Lacustrine organic matter and the Holocene paleoenvironmental record of Lake Albano (central Italy). *Journal of Paleolimnology* 26, 283–292.
- Atahan, P., Grice, K., Dodson, J., 2007. Agriculture and environmental change at Qingpu, Yangtze delta region, China: a biomarker, stable isotope and palynological approach. *The Holocene* 17, 505–514.
- Barnett, E.J., 1994. A Holocene palaeoenvironmental history of Lake Alexandrina, South Australia. *Journal of Paleolimnology* 12, 259–268.
- Belperio, A.P., 1995. Quaternary. In: Drexel, J.F., Preiss, W.V. (Eds.), *The Geology of South Australia, Vol. 2. The Phanerozoic*. South Australia. Geological Survey. Bulletin 54, pp. 219–280.
- Belt, S.T., Allard, W.G., Massé, G., Robert, J.-M., Rowland, S.J., 2000. Highly branched isoprenoids (HBIs): identification of the most common and abundant sedimentary isomers. *Geochimica et Cosmochimica Acta* 64, 3839–3851.
- Belt, S.T., Massé, G., Allard, W.G., Robert, J.-M., Rowland, S.J., 2001a.  $\text{C}_{25}$  highly branched isoprenoid alkenes in planktonic diatoms of the *Pleurosigma* genus. *Organic Geochemistry* 32, 1271–1275.
- Belt, S.T., Massé, G., Allard, W.G., Robert, J.-M., Rowland, S.J., 2001b. Identification of a  $\text{C}_{25}$  highly branched isoprenoid triene in the freshwater diatom *Navicula sclesvicensis*. *Organic Geochemistry* 32, 1169–1172.

Blumer, M., Guillard, R.R.L., Chase, T. 1971. Hydrocarbons in marine phytoplankton. *Marine Biology* 8, 183–189.

Bouloubassi, I., Rullkoter, J., Meyers, P.A. 1999. Origin and transformation of organic matter in Pliocene – Pleistocene Mediterranean sapropels: organic geochemical evidence reviewed. *Marine Geology* 153, 177–197.

Bray, E.E., Evans, E.D., 1961. Distribution of *n*-paraffins as a clue to recognition of source beds. *Geochimica et Cosmochimica Acta* 22, 2–15.

Brenchley, A.J., Gostin, V.A., 1998. Correlation of Holocene lithofacies and biofacies between lakes of the Robe area, southeastern South Australia. *Australasian Quaternary Association Biennial Conference, Fraser Island, Abstracts*, pp. 6–7.

Bronk Ramsey, C., 2010. OxCal 4.1 Manual <<https://c14.arch.oxac.uk/oxcal/>>

Cann, J.R., DeDeckker, P., 1981. Fossil Quaternary and living foraminifera from athalassic (non-marine) saline lakes, southern Australia. *Journal of Paleontology* 55, 660–670.

Cann, J.H., Murray-Wallace, C.V., Belperio, A.P., Brenchley, A.J., 1999. Evolution of Holocene coastal environments near Robe, southeastern South Australia. *Quaternary International* 56, 81–97.

Canuel, E.A., Freeman, K.H., Wakeham, S.G., 1997. Isotopic compositions of lipid biomarker compounds in estuarine plants and surface sediments. *Limnology and Oceanography* 42, 1570–1583.

Castenholz, R.W., 1960. Seasonal changes in the attached algae of freshwater and saline lakes in the Lower Grand Coulee, Washington. *Limnology and Oceanography* 5, 1–28.

Chikaraishi, Y., Naraoka, H., 2003. Compound-specific  $\delta^1\text{D}$ – $\delta^{13}\text{C}$  analyses of *n*-alkanes extracted from terrestrial and aquatic plants. *Phytochemistry* 63, 361–371.

Collister, J.W., Rieley, G., Stern, B., Eglinton, G., Fry, B., 1994. Compound-specific  $\delta^{13}\text{C}$  analyses of leaf lipids from plants with differing carbon dioxide metabolisms. *Organic Geochemistry* 21, 619–627.

Davis, J.B., 1968. Paraffinic hydrocarbons in the sulfate-reducing bacterium *Desulfovibrio desulfuricans*. *Chemical Geology* 3, 155–160.

DeDeckker, P., 1981. Ostracoda from Australian inland waters – notes on taxonomy and ecology. *Proceedings of the Royal Society of Victoria* 93, 43–85.

DeDeckker, P., 1988. An account of the techniques using ostracodes in palaeolimnology in Australia. *Palaeogeography, Palaeoclimatology, Palaeoecology* 62, 463–475.

DeDeckker, P., Geddes, M., 1980. The seasonal fauna of ephemeral saline lakes near the Coorong Lagoon, South Australia. *Australian Journal of Marine and Freshwater Research* 31, 677–699.

Dunlop, R.W., Jefferies, P.R., 1985. Hydrocarbons of the hypersaline basins of Shark Bay, Western Australia. *Organic Geochemistry* 8, 313–320.

Edwards, S., McKirdy, D.M., Bone, Y., Gell, P.A., Gostin, V.A., 2006. Diatoms and ostracods as palaeoenvironmental indicators, North Stromatolite Lake, Coorong National Park, South Australia. *Australian Journal of Earth Sciences* 53, 651–663.

Eglinton, G., Hamilton, R.J., 1967. Leaf epicuticular waxes. *Science* 156, 1322–1335.

Ficken, K.J., Li, B., Swain, D.L., Eglinton, G., 2000. An *n*-alkane proxy for the sedimentary input of submerged/floating freshwater aquatic macrophytes. *Organic Geochemistry* 31, 745–749.

Freeman, K.H., Wakeham, S.G., Hayes, J.M., 1994. Predictive isotopic biogeochemistry: hydrocarbons from anoxic marine basins. *Organic Geochemistry* 21, 629–644.

Fry, B., Wainwright, S.C., 1991. Diatom sources of  $^{13}\text{C}$ -rich carbon in marine food webs. *Marine Ecology Progress Series* 76, 149–157.

Gelpi, E., Schneider, H., Mann, J., Oró, J., 1970. Hydrocarbons of geochemical significance in microscopic algae. *Phytochemistry* 9, 603–612.

Han J., Calvin, M., 1969. Hydrocarbon distribution of algae and bacteria and microbial activity in sediment. *Proceedings of the National Academy of Sciences U.S.A.* 64, 436–443.

Han, J., McCarthy E.D., Van Hoesen W., Calvin, M., Bradley, W.H., 1968. Organic geochemical studies II. A preliminary report on the distribution of aliphatic hydrocarbons in algae, in bacteria and in a recent lake sediment. *Proceedings of the National Academy of Sciences U.S.A.* 59, 29–33.

Henderson, T., 1997. Mineralogy and stable isotope composition of Recent carbonate sediments and waters from five small lakes, south-eastern South Australia. B.Sc. Honours thesis, University of Adelaide (unpublished).

Henderson, W., Reed, W.E., Steel, G., 1972. The origin and incorporation of organic molecules in sediments as elucidated by studies of the sedimentary sequence from a residual Pleistocene lake. In: von Gaertner, H.R., H. Wehner, H. (Eds.), *Advances in Organic Geochemistry 1971*. Pergamon Press, Oxford, pp. 335–352.

Hepplewhite, C., 1994. A study of some biomarker hydrocarbons in organic-rich Holocene sediments of Coorong region, South Australia. B.Sc. Honours thesis, University of Adelaide (unpublished).

Hollander, D.J., McKenzie, J.A., ten Haven, H.L., 1992. A 200 year record of progressive eutrophication in Lake Greifen (Switzerland): implications for the origin of organic-carbon-rich sediments. *Geology* 20, 825–828.

Hollander, D.J., Huc, A.Y., McKenzie, J.A., Hsu, K.J., 1993. Application of an eutrophic lake model to the origin of ancient organic-carbon-rich sediments. *Global Biogeochemical Cycles* 7, 159–179.

Holmes J.W., Waterhouse J.D., 1983. Hydrology. In: Tyler M.J., Twidale C.R., Ling J.K., Holmes J.W. (Eds.), *Natural History of the South East*. Royal Society of South Australia, Adelaide, pp. 49–59.

Irwin, I., Curtis, C., Coleman, M., 1977. Isotopic evidence for source of diagenetic carbonates formed during burial of organic-rich sediments. *Nature* 269, 209–213.

Jaffé, R., Mead, R., Hernandez, M.E., Perlaba, M.C., DiGuida, O.A., 2001. Origin and transport of sedimentary organic matter in two subtropical estuaries: a comparative, biomarker-based study. *Organic Geochemistry* 32, 507–526.

Kenig, F., Huc, A.Y., Purser, B.H., Oudin, J.L., 1989. Sedimentation, distribution and diagenesis of organic matter in a recent carbonate environment, Abu Dhabi, UAE. *Organic Geochemistry* 16, 735–747.

Krull, E., Haynes, D., Lamontagne, S., Gell, P., McKirdy, D., Hancock, G., McGowan, J., Smernik, R., 2009. Changes in the chemistry of sedimentary organic matter within the Coorong over space and time. *Biogeochemistry* 92, 9–25.

Lichtfouse, É., Derenne, S., Mariotti, A., Largeau, C., 1994. Possible algal origin of long chain odd *n*-alkanes in immature sediments as revealed by distributions and carbon isotope ratios. *Organic Geochemistry* 22, 1023–1027.

Martens, K., 1985. The salinity tolerance of *Mytilocypris henricae* (Chapman) (Crustacea, Ostracoda). *Hydrobiologica* 124, 81–83.

Mayewski, P.A., Rohling, E.E., Stager, J.C., Karlen, W., Maasch, K.A., Meeker, L.D., Meyerson, E.A., Gasse F., Van Kreveland, S., Lee-Thorp, J., Rosqvist, G., Rack, F., Staubwasser, M., Schnieder, R.R., Steig, E.J., 2004. Holocene climate variability. *Quaternary Research* 62, 243–255.

Mazzoleni, A.G., 1993. Holocene sedimentology of Old Man Lake, southeastern South Australia. B.Sc. Honours thesis, University of Adelaide (unpublished).

Mazzoleni, A.G., Bone Y., Gostin, V.A., 1995. Cathodoluminescence of aragonitic gastropods and cement in Old Man Lake thrombolites, southeastern South Australia. *Australian Journal of Earth Sciences* 42, 497–500.

McCormac, F.G., Hogg, A.G., Blackwell, P.G., Buck, C.E., Higham, T.F.G., Reimer, P.J., 2004. SHCal04 Southern Hemisphere Calibration, 0–11.0 cal kyr BP. *Radiocarbon* 46, 1087–1092.

McCrea, J.M., 1950. On the isotopic chemistry of carbonates and a paleotemperature scale. *Journal of Chemical Physics* 18, 849–857.

McKirdy, D.M., Hepplewhite, C.J., Michaelsen, B.H., Mazzoleni, A.G., Bone Y., 1995. Origin of sapropels in Holocene lakes of the Coorong region, South Australia. In: Grimalt, J.O., Dorronsoro C. (Eds.), *Organic Geochemistry: Developments and Applications to Energy, Climate, Environment and Human History*. AIGOA, Donostia-San Sebastián, pp. 183–185.

McKirdy, D.M., Spiro, B., Kim, A., Brenchley, A.J., Mazzoleni, A.G., Yu, X., Gostin, V.A., 1999. The environmental evolution of Old Man Lake, southeastern Australia, during the Holocene. 19th International Meeting on Organic Geochemistry, Istanbul, Turkey, Programme and Abstracts, pp. 405–406.

McKirdy, D.M., Brenchley, A.J., Edwards, S., 2002. Lacustrine sapropels as proxies for Late Quaternary environmental change in southeastern Australia. *Geological Society of Australia, Abstracts* 67, 23.

McKirdy, D.M., Hayball, A.J., Warren, J.K., Edwards, D. and von der Borch, C.C., 2010a. Organic facies of Holocene carbonates in North Stromatolite Lake, Coorong region, South Australia. *Cadernos Laboratorio Xeolóxico de Laxe* 35, 127–146.

McKirdy, D.M., Thorpe, C.S., Haynes, D.E., Grice, K., Krull, E.S., Halverson, G.P., Webster, L.J., 2010b. The biogeochemical evolution of the Coorong during the mid- to late Holocene: An elemental, isotopic and biomarker perspective. *Organic Geochemistry* 41, 96–110.

Mead, R., Xu, Y., Chong, J., Jaffé, R., 2005. Sediment and soil organic matter source assessment as revealed by the molecular distribution and carbon isotopic composition of *n*-alkanes. *Organic Geochemistry* 36, 363–370.

Mee, A.C., 2008. Origin, formation and environmental significance of sapropels in shallow Holocene coastal lakes of southeastern Australia. PhD thesis, University of Adelaide (unpublished).

Mee, A.C., McKirdy, D.M., Krull, E.S., Williams, M.A.J., 2004. Geochemical analysis of organic-rich lacustrine sediments as a tool for reconstructing Holocene environmental conditions along the Coorong coastal plain, southeastern Australia. In: Roach I.C. (Ed.), *Regolith 2004*. Cooperative Research Centre for Landscape Environments and Mineral Exploration, Bentley, pp. 247–251.

Mee, A.C., McKirdy, D.M., Williams, M.A.J., Krull, E.S., 2007. New radiocarbon dates from sapropels in three Holocene lakes of the Coorong coastal plain, southeastern Australia. *Australian Journal of Earth Sciences* 54, 825–835.

Meyers, P.A., 2003. Applications of organic geochemistry to palaeolimnological reconstructions: a summary of examples from the Laurentian Great Lakes. *Organic Geochemistry* 34, 261–289.

Meyers, P.A., Lallier-Verges, E., 1999. Lacustrine sedimentary organic matter records of Late Quaternary paleoclimates. *Journal of Paleolimnology* 21, 345–372.

Pell, S.D., Chivas, A.R., 1995. Surface features of sand grains from the Australian Continental Dunefield. *Palaeogeography, Palaeoclimatology, Palaeoecology* 113, 119–132.

Rosen, M. R., Miser, D.E., Warren, J. K., 1988. Sedimentology, mineralogy and isotopic analysis of Pellet Lake, Coorong Region, South Australia. *Sedimentology* 35, 105–122.

Rowland, S.J., Robson, J.N., 1990. The widespread occurrence of highly branched acyclic C<sub>20</sub>, C<sub>25</sub> and C<sub>30</sub> hydrocarbons in recent sediments and biota — A review. *Marine Environmental Research* 30, 191–216.

Rowland, S.J., Allard, W.G., Belt, S.T., Masse, G., Robert, J.-M., Blackburn, S., Frampton, D., Revill, A.T., Volkman, J.K., 2001. Factors influencing the distribution of polyunsaturated terpenoids in the diatom, *Rhizosolenia setigera*. *Phytochemistry* 58, 717–728.

Scalan, R.S., Smith, J.E., 1970. An improved measure of the odd-to-even predominance in the normal alkanes of sediment extracts and petroleum. *Geochimica et Cosmochimica Acta* 34, 611–620.

Spiro, B., Aizenshtat, Z., 1977. Bacterial sulphate reduction and calcite precipitation in hypersaline deposition of bituminous shales. *Nature* 269, 235–237.

Talbot, M.R., Kelts, K., 1990. Paleolimnological signatures from carbon and oxygen isotopic ratios in carbonates from organic carbon-rich lacustrine sediments. In: Katz, B.J. (Ed.), *Lacustrine Basin Exploration – Case Studies and Modern Analogs*. AAPG Memoir 50, pp. 99–112.

Tolun, L., Cagatay, M.N., Carrigan, W.J., 2002. Organic geochemistry and origin of Late Glacial – Holocene sapropelic layers and associated sediments in Marmara Sea. *Marine Geology* 190, 47–60.



- Tyson, R., 1995. *Sedimentary Organic Matter*. Chapman & Hall, London, p. 406.
- Volkman, J.K., Johns, R.B., Gillan, F.T., Perry, G.J., Bavor, H.J. Jr., 1980. Microbial lipids of an intertidal sediment – I. Fatty acids and hydrocarbons. *Geochimica et Cosmochimica Acta* 44, 1133–1143.
- Volkman, J.K., Barrett, S.M., Dunstan, G.A., 1994. C<sub>25</sub> and C<sub>30</sub> highly branched isoprenoid alkenes in laboratory cultures of two marine diatoms. *Organic Geochemistry* 21, 407–414.
- Volkman, J.K., Barrett, S.M., Blackburn, S.I., Mansour, M.P., Sikes, E.L., Gelin, F., 1998. Microalgal biomarkers: a review of recent research developments. *Organic Geochemistry* 29, 1163–1179.
- Von der Borch, C.C., 1976. Stratigraphy and formation of Holocene dolomitic carbonate deposits of the Coorong area, South Australia. *Journal of Sedimentary Petrology* 4, 952–966.
- Von der Borch, C.C., Altmann, M., 1979. Holocene stratigraphy and evolution of the Cooke Plains Embayment, a former extension of Lake Alexandrina, South Australia. *Transactions of the Royal Society of South Australia* 103, 69–78.
- Warren, J. K., 1990. Sedimentology and mineralogy of dolomitic Coorong lakes, South Australia. *Journal of Sedimentary Petrology* 60, 843–858.
- Warren, J. K., 1994. Holocene Coorong lakes, South Australia. In: Gierlowski-Kordesch, E., Kelts, K. (Eds.), *Global Geological Record of Lake Basins*, Vol.1. Cambridge University Press, Cambridge, pp. 387–394.
- Xu, Y., Jaffé, R., Wachnicka, A., Gaiser, E.E., 2006. Occurrence of C<sub>25</sub> highly branched isoprenoids (HBIs) in Florida Bay: paleoenvironmental indicators of diatom-derived organic matter inputs. *Organic Geochemistry* 37, 847–859.
- Yasini, I., Jones, B.G., 1995. Foraminifera and Ostracoda from Estuarine and Shelf

Environments on the Southeastern Coast of Australia. University of Wollongong Press, Wollongong.

Zhang, L., Wang, T., Huang, D., Li, J., Li, X., Shan, M., Wang, X., 1999. Carbon isotopic study of individual n-alkanes in certain modern organisms. Chinese Science Bulletin 44, 1139–1142.

**Table 1** Radiocarbon dates on dissolved inorganic carbon in contemporary water and bulk organic matter in sapropels from Old Man Lake.

Sample	Laboratory code	$\delta^{13}\text{C}$ ‰	Conventional $^{14}\text{C}$ age yr BP	Calibrated $^{14}\text{C}$ age cal yr BP	Reference
Water	OZ1264	0.1	$815 \pm 40$	$700 \pm 30$	Mee et al., 2007
Top of upper sapropel	Wk-5188	-19.3	$2670 \pm 90$	$2660 \pm 230$	This study
	OZH204	-20.8	$3090 \pm 50$	$3270 \pm 70$	Mee et al., 2007
Base of middle sapropel	OZH365	-21.9	$3830 \pm 50$	$4160 \pm 80$	Mee et al., 2007
Base of lower sapropel	Wk-5189	-20.7	$4160 \pm 50$	$4680 \pm 155$	This study
	OZH205	-19.6	$4380 \pm 50$	$4910 \pm 65$	Mee et al., 2007

**Table 2** Bulk geochemistry of organic-rich units in Old Man Lake. Depth intervals measured from compacted cores. S2 = kerogen pyrolysate (mg hydrocarbons/g sediment). HI = hydrogen index (mg S2/g TOC). na = data not available.

Unit	Core	Depth cm	CaCO <sub>3</sub> wt %	TOC wt %	S2	HI	$\delta^{13}\text{C}_{\text{org}}$ ‰	$\delta^{13}\text{C}_{\text{carb}}$ ‰	$\delta^{18}\text{O}_{\text{carb}}$ ‰
Upper sapropel	1	33–40	85	3.2	14	449	−16.9	9.5	3.2
	2	76–83	27	16.4	115	698	−20.2	−0.4	2.4
	3	2–8	80	4.1	19	452	−17.6	8.2	1.6
	4	6–11	60	8.6	46	539	−19.5	6.3	2.5
	5	22–26	53	9.3	75	800	−18.4	4.1	1.9
Middle sapropel	1	60–66	74	6.0	24	397	−20.8	0.7	3.3
	2	95–103	30	19.6	116	595	−21.9	1.9	2.8
	3	16–21	57	9.5	27	278	−21.0	2.0	2.5
	4	18–23	66	6.4	35	556	−21.9	−2.7	1.5
	5	33–38	67	10.0	33	334	−21.9	−0.7	2.9
Lower sapropel	1	88–93	62	7.6	40	526	−19.5	1.0	2.8
	2	115–128	60	8.6	37	433	−20.8	0.7	2.7
	3	32–39	67	6.9	33	474	−19.8	2.6	1.6
	4	27–33	68	7.8	39	506	−20.3	0.4	2.0
	5	47–54	60	10.3	51	498	−20.6	1.1	2.6
Upper humic	1	144–151	na	23.9	25	106	−26.7	0.6	1.2
	4	180–188	8	29.1	61	210	−24.4	0.8	0.5
	5	130–138	18	14.3	26	179	−25.8	−0.7	0.7
Lower humic	4	194–201	11	1.5	7	na	−26.0	na	na
	5	170–181	4	1.6	2	108	−25.3	−1.7	−0.1

**Table 3** EOM and aliphatic hydrocarbon yields and *n*-alkane and highly branched isoprenoid (HBI) signatures of organic-rich units in Old Man Lake. CPI = carbon preference index for *n*-C<sub>23</sub>–C<sub>32</sub> (Bray and Evans, 1961). OEP = odd/even predominance (Scalan and Smith, 1970) for *n*-C<sub>29</sub>. *Paq* = [*n*-C<sub>23</sub> + *n*-C<sub>25</sub>]/[*n*-C<sub>23</sub> + *n*-C<sub>25</sub> + *n*-C<sub>29</sub> + *n*-C<sub>31</sub>] (Ficken et al., 2000). The HBI 25:1 quantified is the major isomer. \* Measured from silicalite adduct. nd = HBIs not detected.

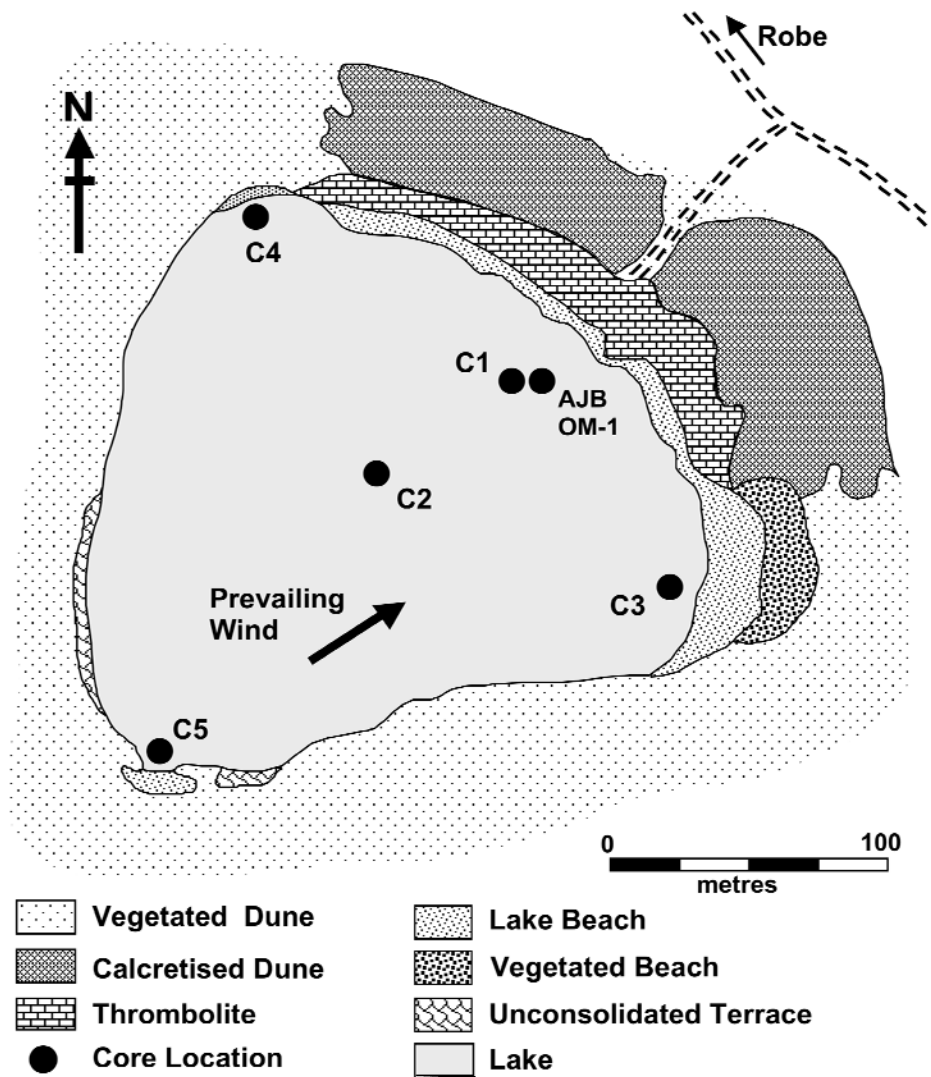
Unit	Core	EOM ppm	Aliph ppm	Max <i>Paq</i>	<i>n</i> -Alkanes CPI OEP		HBI 25:1/20:0	HBI 25:1/ <i>n</i> -C <sub>31</sub>	
Upper sapropel	5	10945	361	31	8.9	5.3	0.34	240*	1.75
Middle sapropel	1	4377	131	31	9.9	13.7	0.42	22.6*	0.77
	2	10886	337	31	5.7	14.2	0.31	28.4*	0.61
	3	7917	223	31	11.5	13.9	0.51	9.7	0.58
	4	6426	129	31	11.8	4.7	0.33	2.4	0.27
	5	5779	110	31	9.3	11.6	0.40	1.7*	0.23
Lower sapropel	5	7618	175	31	8.4	11.4	0.34	12.0*	0.65
Upper humic	5	4235	131	25	16.6	26.5	0.83	nd	0.01
Lower humic	5	945	20	31	3.2	12.0	0.31	nd	nd

**Table 4** Carbon isotopic signatures ( $\delta^{13}\text{C}$ , ‰) of selected aliphatic hydrocarbons in sapropels from Old Man Lake. HBI 25:1 is the most abundant isomer (peak D in Fig. 8).

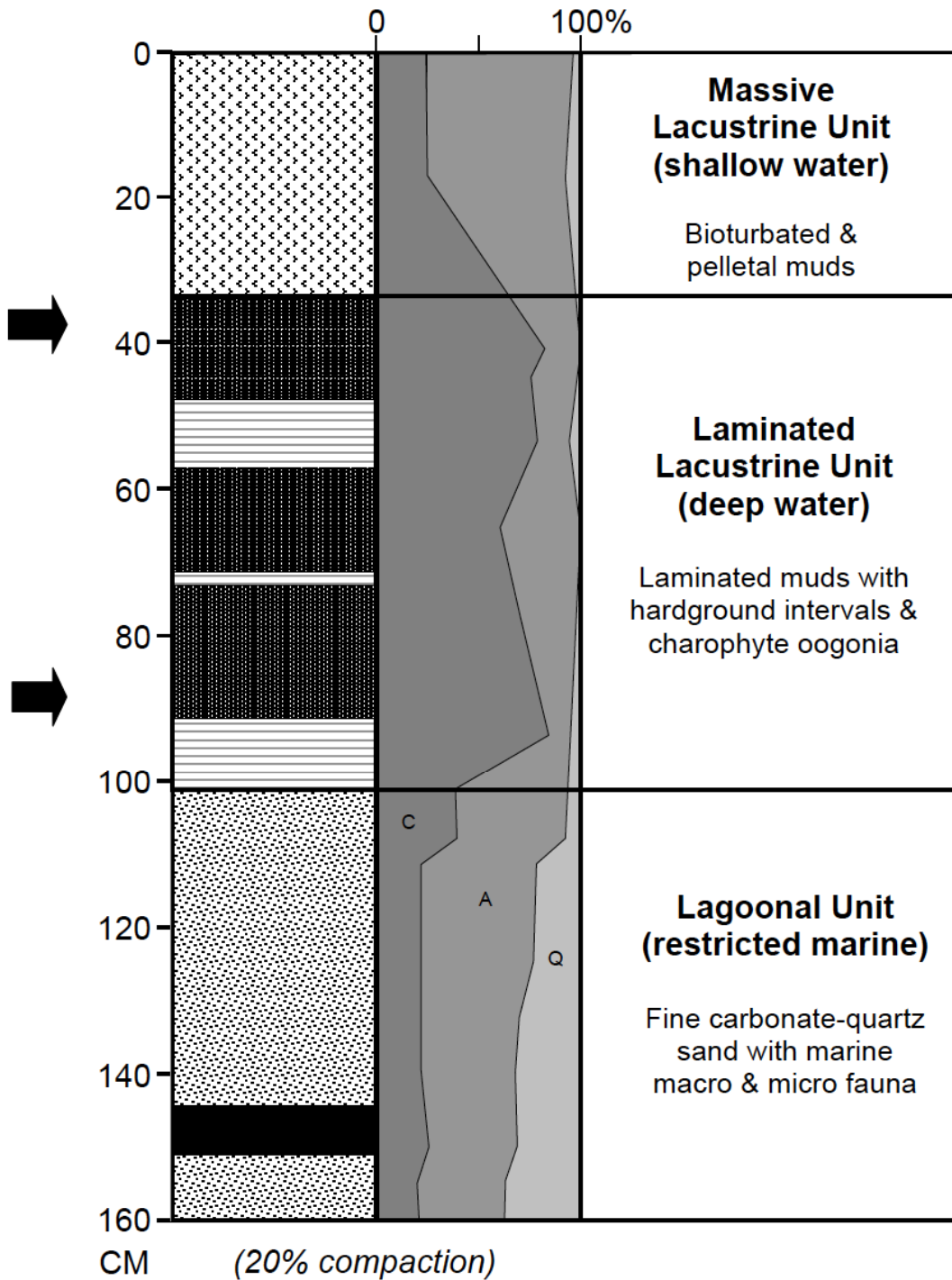
Unit	Core	<i>n</i> -Alkanes					HBI 25:1	
		23 33	25	27	29	31		
Upper sapropel	5	-25.5	-28.2	-25.1	-28.2	-30.6	-29.2	-24.8
Middle sapropel	1	-23.9	-27.8	-25.2	-29.2	-31.2	-30.0	-23.1
	2	-25.6	-28.3	-25.6	-29.2	-31.5	-30.6	-25.8
	5	-27.8	-30.1	-26.9	-29.6	-31.1	-31.0	-23.7
Lower sapropel	5	-25.5	-28.3	-25.7	-29.5	-32.1	-30.1	-24.3

**Figure 1** Location of Old Man Lake and other lacustrine depocentres on the Coorong coastal plain, southeastern South Australia (modified from Mee et al., 2007; reproduced with permission of the Geological Society of Australia).



**Figure 2** Geological map of Old Man Lake showing surface geology and core locations.

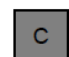
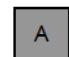
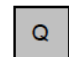


**Figure 3** Lithostratigraphy and mineralogy of core AJB OM-1. Arrows indicate horizons sampled for AMS radiocarbon dating. Note that cores 4 and 5, located on the western side of the lake, penetrated a second humic layer.



**Organic-Rich Layers**

-  Sapropelic
-  Humic

-  Calcite
-  Aragonite
-  Quartz



**Figure 4** Ostracod biostratigraphy and palaeoecology of Core AJB OM-1.

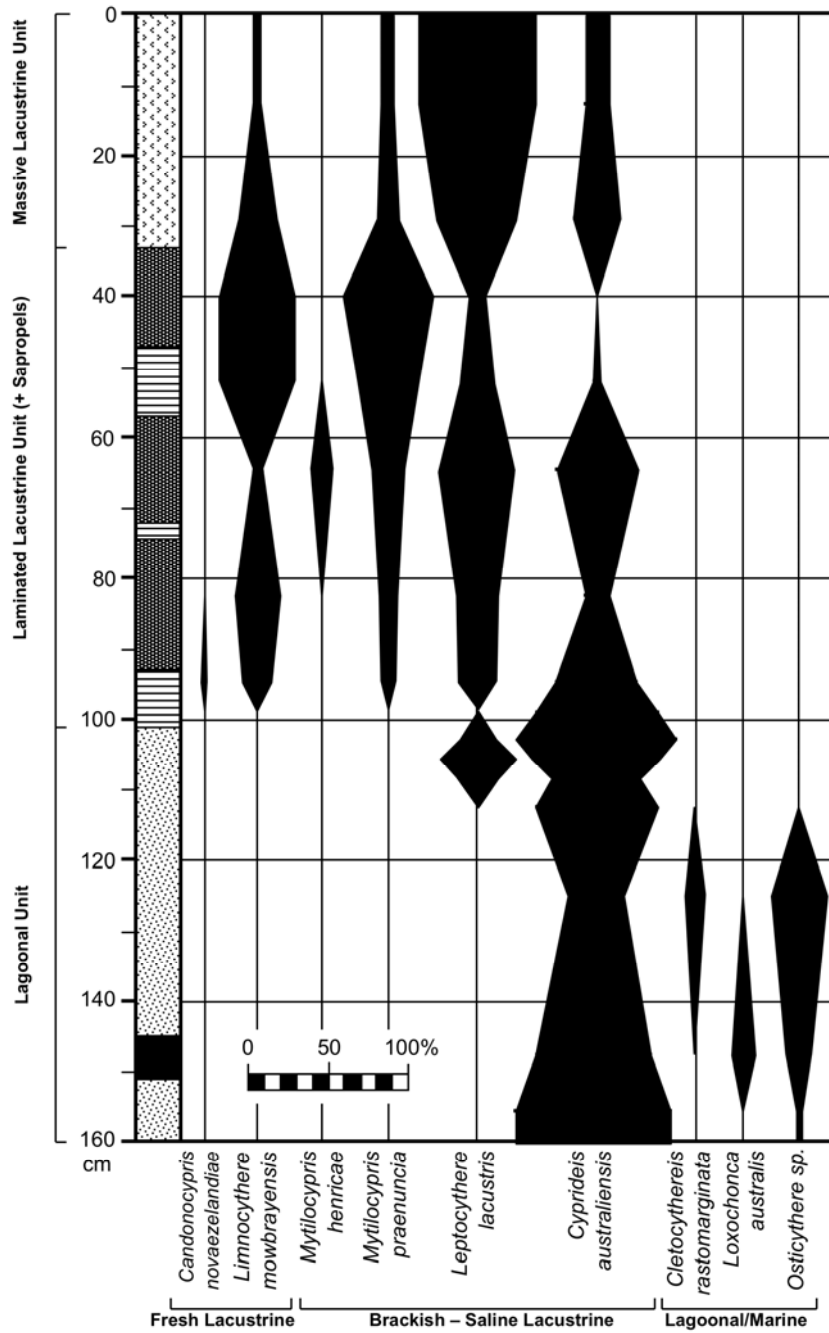


**Figure 5** Cross plot of S2 versus TOC illustrating the organic facies of Old Man Lake and their comparison with a sapropel unit in North Stromatolite Lake (based on data from McKirdy et al., 2010a).

**Figure 6** Cross plot of  $\delta^{13}\text{C}$  versus  $\delta^{18}\text{O}$  for carbonate in organic-rich sediments of Old Man Lake. Field for methanic carbonate after Talbot and Kelts (1990). Note that the carbonates associated with sapropels have higher  $\delta^{18}\text{O}$  values than those in the humic facies, indicating a higher degree of evaporation of the water from which they precipitated.

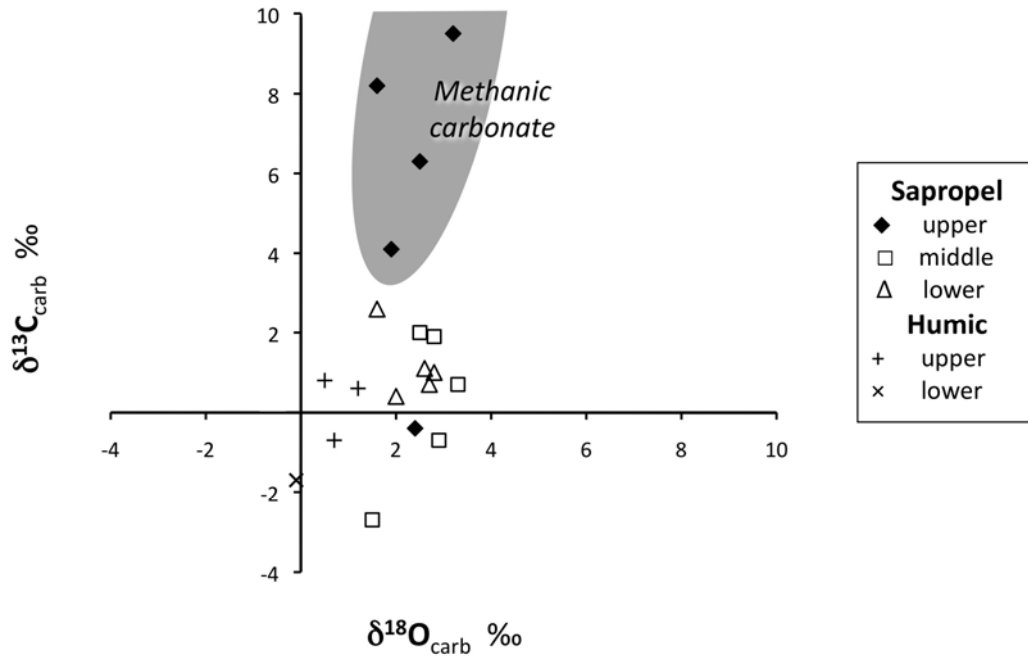


**Figure 7** Total ion current chromatograms of aliphatic hydrocarbons from a) middle sapropel in Core 2 and b) lower humic interval in Core 5, Old Man Lake. Numbers = chain length of *n*-alkanes. HBI 20:0 = 2,6,10-trimethyl-7-(3-methylbutyl)-dodecane. HBI 25:1 = isomers of 2,6,10-trimethyl-7-(3,7-dimethyloctyl)-dodecene.

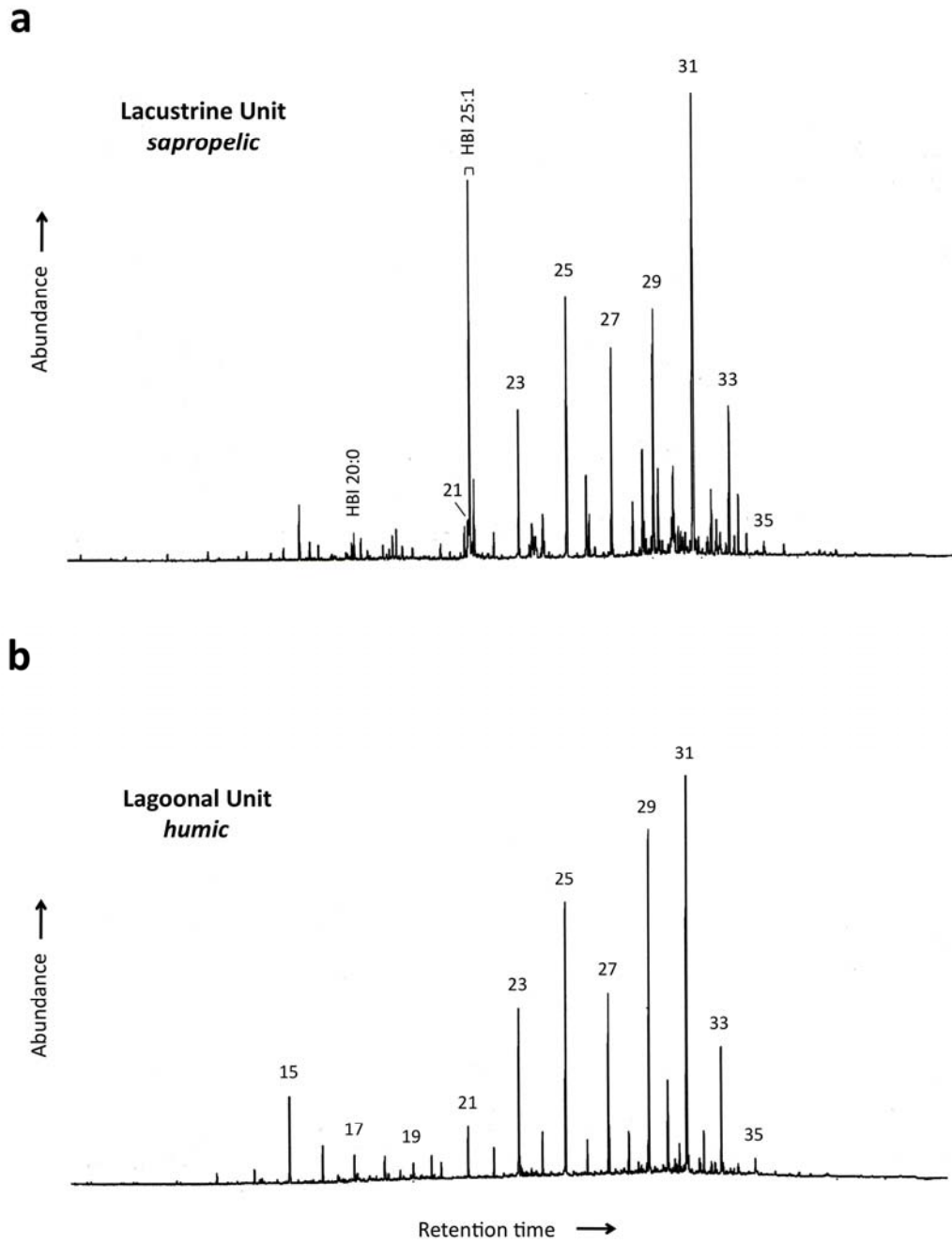


**Figure 8** Mass spectra of C<sub>25</sub> highly branched isoprenoid hydrocarbons in middle sapropel from Core 3, Old Man Lake. Isomers D, E and F = alkenes; isomer G = alkadiene.

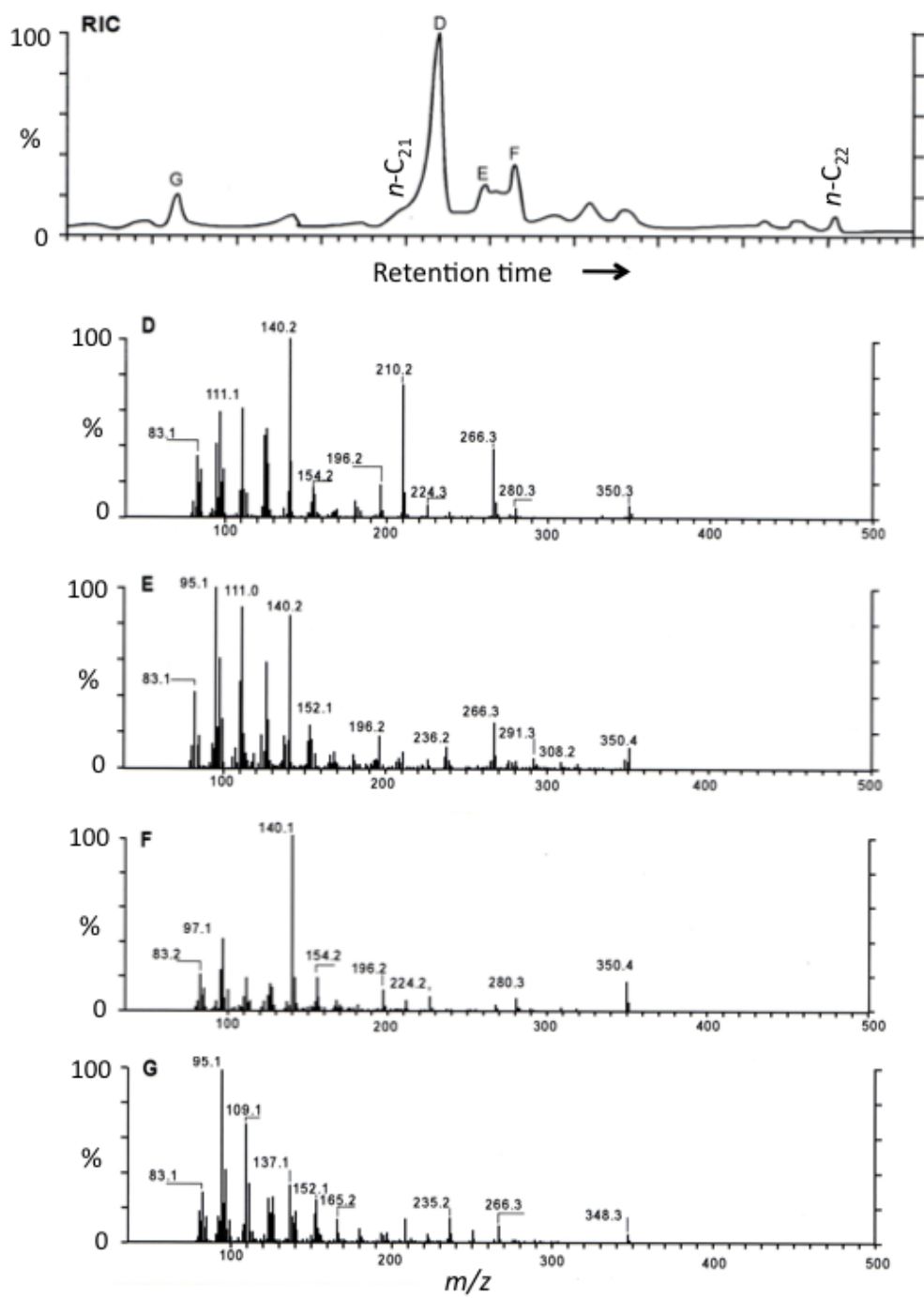
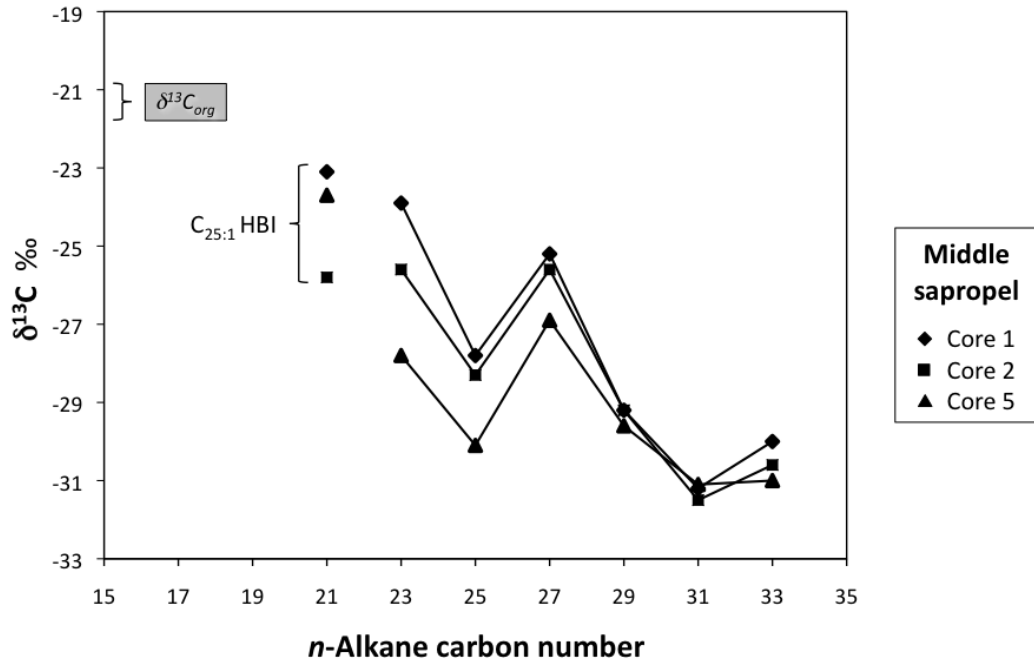


**Figure 9** Carbon isotopic signatures of total organic carbon ( $C_{org}$ ),  $C_{25:1}$  highly branched isoprenoid alkene (dominant isomer) and odd-carbon-numbered  $n$ -alkanes in selected sapropel samples from Old Man Lake.

**a**



**b**

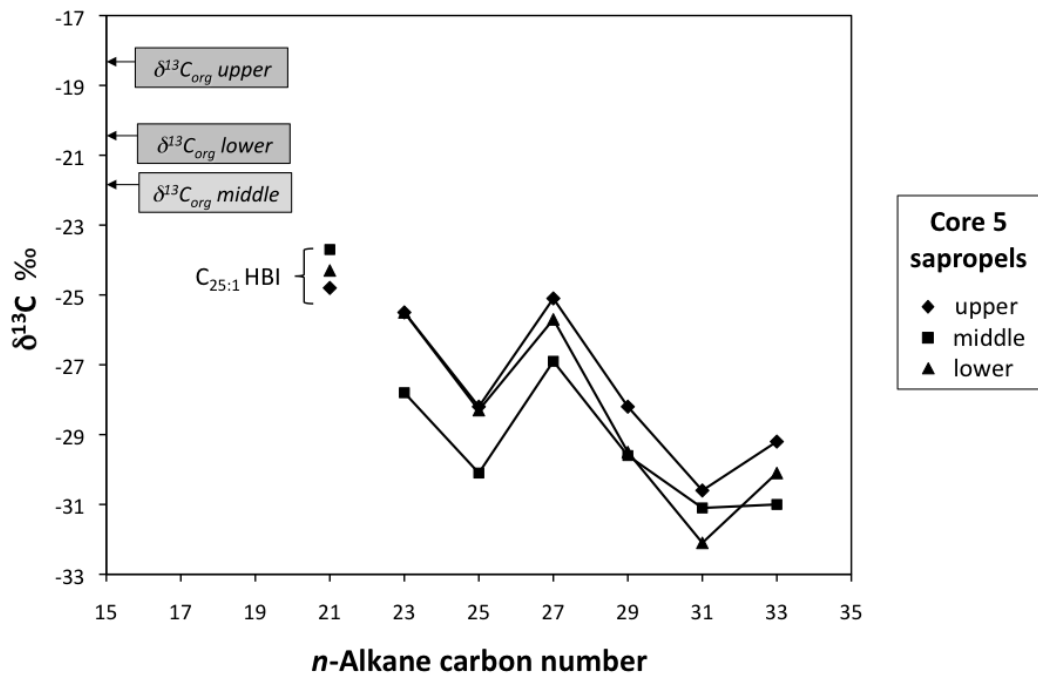


**Figure 10** Carbon isotopic signatures of total organic carbon ( $C_{org}$ ),  $C_{25:1}$  highly branched isoprenoid alkene (dominant isomer) and odd-carbon-numbered  $n$ -alkanes in sediment samples recording two contrasting trophic states of Lake Koucha, Tibet (based on data from Aichner et al., 2010).

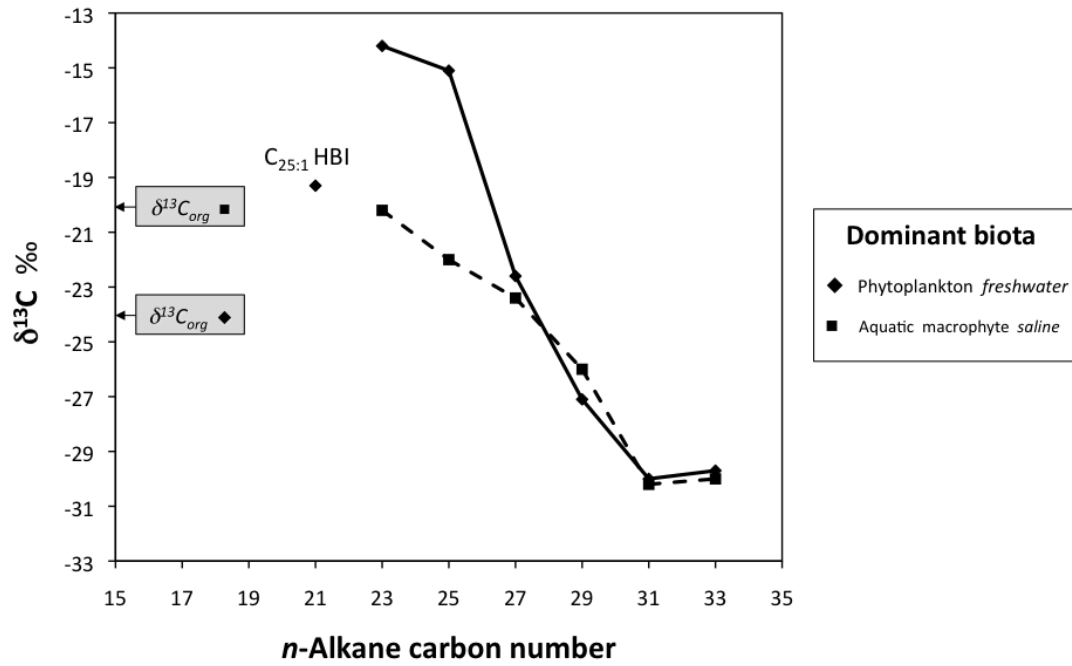


**Figure 11** Cross-plot of hydrogen index versus  $\Delta^{13}\text{C}$  for sapropels in Old Man Lake.  $\Delta^{13}\text{C} = \delta^{13}\text{C}_{\text{carb}} - \delta^{13}\text{C}_{\text{org}}$  (per mil relative to V-PDB). Numerals = core numbers. L, M and U = trends of increasing organic preservation across lake during deposition of the lower, middle and upper sapropel units, respectively. Note the lack of lateral and secular uniformity within the sapropels. Interpretation based on eutrophic lake model of Hollander et al. (1992, 1993).

